
REPORT No. 323

**FLOW AND FORCE EQUATIONS FOR A BODY
REVOLVING IN A FLUID**

**By A. F. ZAHM
Aerodynamical Laboratory
Bureau of Construction and Repair, U. S. Navy**

CONTENTS

	Page		Page
SUMMARY.....	411	PART III. ZONAL FORCE AND MOMENT	
PART I. INTRODUCTION.....	412	ON HULL FORMS.....	427
Steady-flow method.....	412	Pressure loading.....	427
General formulas for velocity components.....	413	Zonal force.....	428
Surface velocity.....	413	Zonal moment.....	428
Zonal forces and moments.....	413	Correction factors.....	428
Geometrical formulas.....	414	PART IV. RESULTANT FORCE AND MOMENT.....	429
Conventions.....	415	Body in free space.....	429
PART II. VELOCITY AND PRESSURE.....	416	Reactions of fluid.....	429
(A) Bodies in Simple Rotation.....	416	Combination of applied forces.....	431
Elliptic cylinder.....	416	Hydrokinetically symmetric forms.....	432
Prolate spheroid.....	418	Examples.....	432
Ellipsoid.....	422	Theory vs. experiment.....	433
(B) Bodies in Combined Translation and Rotation.....	422	Correction factors.....	435
Most general motion.....	422	PART V. POTENTIAL COEFFICIENTS—INERTIA COEFFICIENTS.....	436
Yawing flight.....	422	Green's integrals.....	436
Flow inside ellipsoid.....	424	Potential coefficients.....	436
Potential coefficients.....	426	Inertia coefficients.....	436
Relative velocity and kinetic pressure.....	426	Limiting conditions.....	437
		Physical meaning of the coefficients.....	437
		SYMBOLS USED IN THE TEXT.....	438
		REFERENCES.....	438
		TABLES AND DIAGRAMS.....	439

REPORT No. 323

FLOW AND FORCE EQUATIONS FOR A BODY REVOLVING IN A FLUID

IN FIVE PARTS

By A. F. ZAHM

SUMMARY

This report, submitted to the National Advisory Committee for Aeronautics for publication, is a slightly revised form of U. S. Navy Aerodynamical Laboratory Report No. 380, completed for the Bureau of Aeronautics in November, 1928. The diagrams and tables were prepared by Mr. F. A. Loudon; the measurements given in Tables 9 to 11 were made for this paper by Mr. R. H. Smith, both members of the Aeronautics Staff.

Part I gives a general method for finding the steady-flow velocity relative to a body in plane curvilinear motion, whence the pressure is found by Bernoulli's energy principle. Integration of the pressure supplies basic formulas for the zonal forces and moments on the revolving body.

Part II, applying this steady-flow method, finds the velocity and pressure at all points of the flow inside and outside an ellipsoid and some of its limiting forms, and graphs those quantities for the latter forms. In some useful cases experimental pressures are plotted for comparison with theoretical.

Part III finds the pressure, and thence the zonal force and moment, on hulls in plane curvilinear flight.

Part IV derives general equations for the resultant fluid forces and moments on trisymmetrical bodies moving through a perfect fluid, and in some cases compares the moment values with those found for bodies moving in air.

Part V furnishes ready formulas for potential coefficients and inertia coefficients for an ellipsoid and its limiting forms. Thence are derived tables giving numerical values of those coefficients for a comprehensive range of shapes.

REPORT No. 323

FLOW AND FORCE EQUATIONS FOR A BODY REVOLVING IN A FLUID

PART I

INTRODUCTION

STEADY-FLOW METHOD.—In some few known cases one can compute the absolute particle velocity q' at any point (x, y, z) of the flow caused by the rotation of a body, say with uniform angular speed Ω , in an infinite inviscid liquid otherwise still. Thence, since q' is unsteady at (x, y, z) , the instantaneous pressure there is found by Kelvin's formula $p_0/\rho = -\partial\phi/\partial t - q'^2/2$, p_0 being the supervacuo pressure there, and ϕ the velocity potential.

Otherwise superposing upon said body and flow field the reverse speed $-\Omega$, about the same axis, gives the same relative velocity q but which now is everywhere a steady space velocity. In the body's absence the circular flow speed at the radial distance R would be $q_0 = -\Omega R$.¹ If the fixed body's presence lowers the speed at (x, y, z) from q_0 to q , it obviously begets there the superstream pressure

$$p = \frac{1}{2}\rho(q_0^2 - q^2) \quad (1)$$

or in dimensionless form, a being some fixed length in the body,

$$\frac{p}{\frac{1}{2}\rho a^2 \Omega^2} = \frac{R^2}{a^2} (1 - q^2/q_0^2) \quad (1)_2$$

The present text finds p by this steady-flow method only, and applies it to streams about various forms of the ellipsoid and its derivatives.

The superposed circular flow, $q_0 = -\Omega R = -\partial\psi/\partial R$, has the stream-function

$$\psi = \frac{1}{2}\Omega R^2 \quad (2)$$

which, for rotation about the z axis, plots as in Figure 4. This flow has no velocity potential, since $\partial\psi/\partial R \neq 0$.

GENERAL FORMULAS FOR VELOCITY COMPONENTS.—In plane flow,³ as is known, a particle at any point (x, y) of a line s drawn in the fluid has the tangential and normal velocity components

$$q_t = \frac{\partial\phi}{\partial s} = -\frac{\partial\psi}{\partial n} \quad q_n = \frac{\partial\phi}{\partial n} = \frac{\partial\psi}{\partial s} \quad (3)$$

¹ This velocity entails the centrifugal pressure $p_0 = \rho\Omega^2 R^2/2$ at all distances, $R = \sqrt{x^2 + y^2}$ from the rotation axis of the circular stream, here assumed to be constrained by a coaxial closed cylinder infinitely large. To the dynamic pressure $p_0 + p$ may also be added any arbitrary static pressure such as that due to weight or other impressed force.

² At any surface point of the body q is the velocity of wash or slip, whether the body moves or not; it is $q' - q''$, the difference of the tangential space velocities of the fluid and surface point. If the body is fixed $q'' = 0$, $q = q'$.

³ Plane flow, viz two-dimensional flow, literally means flow in a plane; the term applies also to space flow that is the same in all parallel planes.

where δs , δn are elements along the line and its normal. As usual, q_t , q_n are reckoned positive respectively along δs , δn positive; e. g. Figure 2. The components along x , y are

$$u = \frac{\partial \varphi}{\partial x} = \frac{\partial \psi}{\partial y} \quad v = \frac{\partial \varphi}{\partial y} = -\frac{\partial \psi}{\partial x} \quad (4)$$

In solid flow (3), (4) still hold for φ , and further $w = \partial \varphi / \partial z$. In general, $q^2 = u^2 + v^2 + w^2 = q_t^2 + q_n^2$. At any point of a surface drawn in the fluid q_t is taken in the plane of q and q_n . All these velocities are referred to fixed space.

SURFACE VELOCITY.—A fixed body in any stream, since $q_n = 0$, has the surface flow velocity $q = q_t$, which put in (1) determines the surface pressure.

At any surface point of an immersed moving body q_n is the same for body and fluid, hence is known from solid kinematics. Thus, if the body is any cylinder rotating as in Figure 1,

$$q_n = -\Omega R \, dR/ds = \Omega R \sin(\theta - \beta) = \Omega h_1 = \Omega(mx - ly) \quad (5)$$

where the symbols are as defined in Figures 1, 2.

More generally, for any surface with velocities Ω_x , Ω_y , Ω_z about the axes x , y , z ,

$$q_n = (ny - mz)\Omega_x + (lz - nx)\Omega_y + (mx - ly)\Omega_z \quad (6)$$

where l , m , n are the direction cosines of the surface normal, as in (13₁).

If at the same time the body has translation components, U , V , W along x , y , z , (6) must be increased by $lU + mV + nW$, giving

$$q_n = l(U + z\Omega_y - y\Omega_z) + m(V + x\Omega_z - z\Omega_x) + n(W + y\Omega_x - x\Omega_y) \quad (7)$$

But (5), (6), (7) express q_n only at the model's surface.

Equations (1) to (7) obtain whether the fluid is inside or outside the body.

ZONAL FORCES AND MOMENTS.—For any cylinder spinning about z , as in Figure 1 or 5, surface integration of p gives, per unit of z -wise length, the zonal⁴ forces and moment, respectively,

$$X = \int p \, dy \quad Y = \int p \, dx \quad N = \int p \, r \, dr \quad (8)$$

where $p \, dy$, $p \, dx$ are the x , y components of the elementary surface force $p \, ds$, and r is the radius vector of (x, y) . To derive N we note that $p \, ds$ has components $p \, r \, d\beta$, $p \, dr$ along and across r . Having no moment, $p \, r \, d\beta$ can be ignored, leaving only $p \, dr$ with arm r . Thus, $2N = \int p \, d(r^2)$, which varies as the area of the graph of p versus r^2 .

A surface of rotation about x , spinning about its z axis, has zonal forces

$$X = \iint p \, dy \, dz \quad Y = \iint p \, dx \, dz \quad (9)$$

⁴A zone is any part of the surface bounded by two parallel planes; in this text they are assumed normal to z , and the zone has the bounding planes $x=0$, $x=\pm x_1$; in Part III other planes are used; e. g. $x=x_1$, $x=a$.

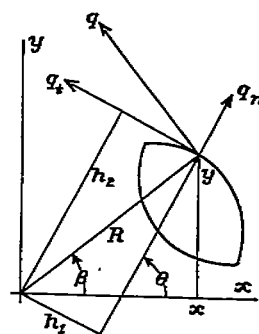


FIGURE 1.—Component velocities q_n , q_t of surface point of any rigid cylinder having angular speed Ω about any axis parallel to its length. $q_n = \Omega h_1$; $q_t = \Omega h_2$. $h_1 = R \sin(\theta - \beta) = -R \, dR/ds = mx - ly$, $1, m$ being direction cosines of the normal to the contour element ds at (x, y) . If the body rotates in a fluid, $q_n = \partial \psi / \partial s = \partial \varphi / \partial n$. At any surface point q_n is the same for body and fluid; q_t different except at points of no slippage

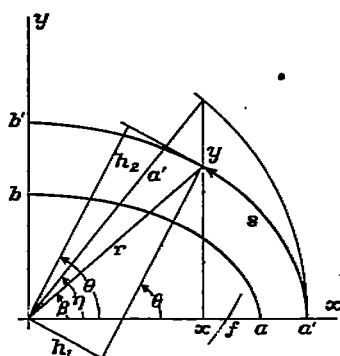


FIGURE 2.—Geometric data for confocal ellipses. $x = a' \cos \eta = r \cos \beta$; $y = b' \sin \eta = r \sin \beta$; $b'/a' \tan \theta = \tan \eta = a'/b' \tan \beta = a'/y$; $h_1 = r \sin(\theta - \beta)$; $h_2 = r \cos(\theta - \beta)$. $f = ae = a' e'$, $e = \sqrt{1 - b^2/a^2}$ being eccentricity of ab

The partial derivatives of λ are

$$\frac{\partial \lambda}{\partial x} = 2lh_2 \quad \frac{\partial \lambda}{\partial y} = 2mh_2 \quad \frac{\partial \lambda}{\partial z} = 2nh_2 \quad \frac{\partial \lambda}{\partial n} = 2h_2 \quad (14)$$

More generally for any surface $f(x, y, z) = 0$, one knows

$$l = j \frac{\partial f}{\partial x} \quad m = j \frac{\partial f}{\partial y} \quad n = j \frac{\partial f}{\partial z} \quad j = \left[\left(\frac{\partial f}{\partial x} \right)^2 + \left(\frac{\partial f}{\partial y} \right)^2 + \left(\frac{\partial f}{\partial z} \right)^2 \right]^{-1/2} \quad (13_1)$$

and the distance from the origin to the tangent plane at (x, y, z) is

$$h_2 = lx + my + nz = r \cos \gamma \quad (12)$$

γ being the angle between the radius vector r and the normal.

CONVENTIONS.—In all the text x, y, z have the positive directions shown in Figure 3, as also have the x, y, z components of velocity, acceleration, force, linear momentum. The angular components about x, y, z of velocity, acceleration, moment, momentum are positive in the respective directions y to z , z to x , x to y . The positive direction of a plane closed contour s is that followed by one going round it with the inclosure on his left, as in Figure 2; the positive direction of the normal n is from left to right across s ;

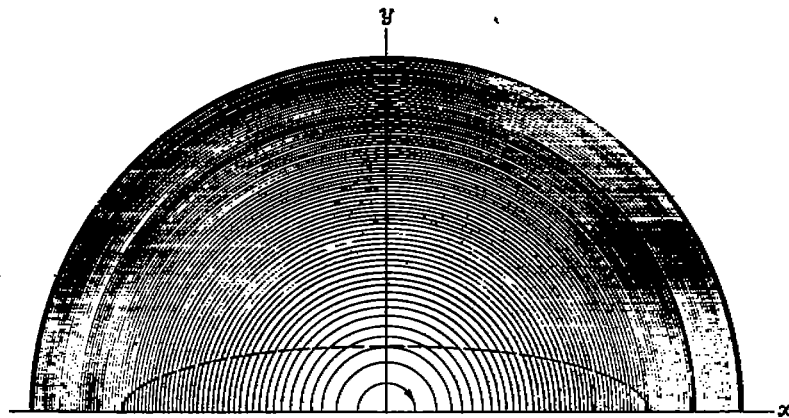


FIGURE 4.—Streamlines for $\psi = \frac{1}{2} \Omega R^2$, with increments $\Delta \psi = 0.2$, for fluid rotating with uniform angular velocity $\Omega = -1$

and $\delta s, \delta n$ determine the positive directions of the tangential and normal flow velocities q_s, q_n , as previously stated. For a closed surface δn is positive outward and δs is positive in the direction of one walking on the outer surface with n on his left.

The word "displaced fluid," used in treating the motion of a submerged body, usually means fluid that would just replace the body if the latter were removed.

REPORT No. 323

FLOW AND FORCE EQUATIONS FOR A BODY REVOLVING IN A FLUID

PART II VELOCITY AND PRESSURE

(A) BODIES IN SIMPLE ROTATION

ELLIPTIC CYLINDER.—For an endless elliptic cylinder, of semiaxes $a, b, c (= \infty)$, rotating about c with angular speed Ω , in an infinite inviscid liquid, otherwise still, one knows¹

$$\varphi = -m' \Omega xy = -\frac{1}{2} m' \Omega a' b' \sin 2\eta \quad \psi = -\frac{1}{2} m' \Omega a' b' \cos 2\eta \quad (15)$$

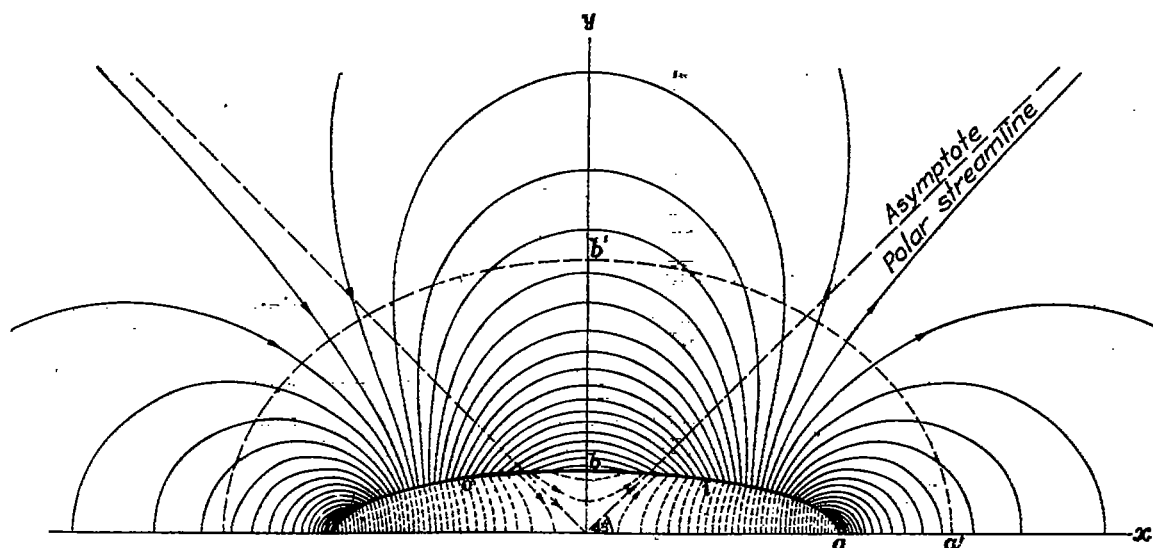


FIGURE 5.—Streamlines for endless elliptic cylinder rotating about its long axis with uniform angular velocity Ω ; shows $\psi = -\frac{1}{2} m' \Omega a' b' \cos 2\eta$ with increments $\Delta \psi = .2, \Omega = 1$. For inside fluid, $\psi = -\frac{1}{2} \frac{a^2 - b^2}{a^2 + b^2} \Omega (x^2 - y^2)$

the geometric symbols being as in Figure 2. For any outer confocal $a'b'$ the potential coefficient has the constant value

$$m'_c = (a+b)^2(a'-b')/2a'b'(a'+b') \quad (16)^2$$

On the model's surface $a' = a, b' = b$; $m'_c = (a^2 - b^2)/2ab$.

The equipotential lines on either surface ab or $a'b'$ are its intersections with the corresponding family of hyperbolic cylinders $xy = -\varphi/m' \Omega = \text{const.}$ Normal to the equipotentials are the streamlines $\psi = \text{const.}$ Graphs for $\psi = 0, 0.2, 0.4$, etc., are shown in Figure 5 for a model having $a/b = 4$. They are instantaneous streamlines, and form with the model a constant pattern in uniform rotation about c in said infinite liquid.

At any outer confocal $a'b'$ the velocity components are, if $\kappa = m' a' b' \Omega$,

$$q'_t = \frac{\partial \varphi}{\partial s} = -\kappa \cos 2\eta \frac{d\eta}{ds} \quad q'_n = \frac{\partial \psi}{\partial s} = \kappa \sin 2\eta \frac{d\eta}{ds} = -q'_t \tan 2\eta \quad (17)$$

¹ Proofs of (15), (23), (29), (40) are found in books; e. g., Lamb §§ 72, 106, 110, 115, 5th ed., except that Lamb reverses the sign of φ, ψ .

² Equivalent to (16) is $m'_c = \left(\frac{e' e' + \sqrt{1-e'^2}}{e' e' + \sqrt{1-e'^2}} \right) \frac{e'^2}{2\sqrt{1-e'^2}}$, e, e' being the eccentricities of $ab, a'b'$. On ab this becomes $m'_c = e/\sqrt{1-e^2}$. See (49) for the six potential coefficients $m_a, m_b, m_c, m'_a, m'_b, m'_c$, in the value of φ for more general motion.

where $d\eta/ds = 1/a' \sqrt{1 - e'^2 \cos^2 \eta}$, as one easily finds. Alternative to (17) are

$$q'_t = -m'_e \Omega_c \frac{d}{ds} xy = -m'_e \Omega_c r \cos(\theta + \beta) \quad q'_n = -q'_t \tan 2\eta \quad (17_1)$$

Thus for $\eta = 0, 45^\circ, 90^\circ$ (17) and (17₁) give $q'_t/\Omega_c = -m'_e a', 0, m'_e b'$. At the model's surface, where $m'_e = (a'^2 - b'^2)/2ab$, (17₁) become

$$q'_t = -\frac{a'^2 - b'^2}{2ab} \Omega_c r \cos(\theta + \beta) \quad q'_n = \Omega_c r \sin(\theta - \beta) \quad (17_2)$$

the latter being $h_1 \Omega_c$, as in (5).

Where $q'_t = 0$, or $\cos \eta = 1/\sqrt{2}$, viz, at the stream poles, clearly $x = a'/\sqrt{2}$, $y = b'/\sqrt{2}$,

$$x^2 - y^2 = a'^2 e^2 / 2 \quad (18)$$

a rectangular hyperbola. (18) is the instantaneous polar streamline, e. g., Figure 5, orthogonal to all the confocal ellipses. Its asymptotes are $y = \pm x$; its vertices are at $x = \pm ae/\sqrt{2}$; it cuts each ellipse where $x/y = a'/b'$, viz, on the diagonals of the circumscribed rectangle. For an endless thin plate of width $2a$ the poles are at $y = 0$, $x = \pm a/\sqrt{2}$.

Superposing $-\Omega_c$ on the body and fluid, and using (2), changes (15) to

$$\psi = \frac{1}{2} (r^2 - m'_e a' b' \cos 2\eta) \Omega_c \quad (19)$$

Its graph, with $\Delta\psi = 0.2$, gives the streamlines in Figure 6 for the flow $\Omega_c = -1$ round a fixed cylinder having $a/b = 4$. About the point (0, 1.45) in Figure 6, is a whirl separated from the outer flow by the streamline $\psi = 4.25$. This line abuts on the model at the inflow points i, i ; spreads round it and emerges at the outflow points o, o .³ The streamlines for an endless thin rectangle having $b = 0$, $e = 1$, are similar to those of Figure 6, but infinitely crowded at the edges.

The superposed particle velocity $-\Omega_c r$ contributes to (17₁)

$$q''_t = -\Omega_c r \cos(\theta - \beta) = -h_2 \Omega_c \quad q''_n = -\Omega_c r \sin(\theta - \beta) = -h_1 \Omega_c \quad (20)$$

also $q''_n = q''_t \tan(\theta - \beta)$. Adding (17₁) and (20) gives the components $q_t = q'_t + q''_t$, $q_n = q'_n + q''_n$, of the resultant flow velocity at any field point. One notes that (20) are the reverse of q_t, q_n in Figure 1.

In particular $q_n = 0$ on the fixed model and x, y axes; hence there

$$q/a\Omega_c = -\frac{r}{a} [m'_e \cos(\theta + \beta) + \cos(\theta - \beta)] \quad q/q_o = m'_e \cos(\theta + \beta) + \cos(\theta - \beta) \quad (21)$$

Thus $q/q_o = 1 + m'_e$ on the x axis; $1 - m'_e$ on the y axis; and 1 at ∞ where $m'_e = 0$. The dashed line in Figure 6 gives $q/a\Omega_c = -(1 - m'_e)y/a$ for points on the y axis; it crosses y at the whirl center where $q = 0$, viz, where $m'_e = 1$. By (16) $m'_e \geq 1$ for the surface of any model having $a/b \geq 1 + \sqrt{2}$; and there is no whirl if $a/b < 1 + \sqrt{2}$. Figure 7 shows $q/a\Omega_c$ for the surface of a model having $a/b = 4$, $m'_e = (a^2 - b^2)/2ab = 15/8$.

Putting q^2/q_o^2 of (21) in (1₁), where $r^2/a^2 = \cos^2 \eta / \cos^2 \beta$, gives

$$p/\frac{1}{2} \rho a^2 \Omega_c^2 = (1 - [m'_e \cos(\theta + \beta) + \cos(\theta - \beta)]^2) \cos^2 \eta / \cos^2 \beta \quad (22)$$

which is graphed in Figure 7 for a model having $a/b = 4$.

Integrating $p/\frac{1}{2} \rho a^2 \Omega_c^2$, as in (8), gives for an inviscid liquid $Y = 0 = N$; $X \neq 0$. Figure 7 delineates X for this case.

³ The points i, o are identical with those in Figure 5; viz, where the slip speed g in (21) is zero; they are called stop points, stagnation points, etc.

For the surface of an endless flat plate ($b=0$, $c=\infty$) fixed in the stream $-\Omega_c$, clearly $m'_c = a/2b$ and generally $r \cos(\theta - \beta) = 0$; hence (21) gives

$$q/a\Omega_c = -\frac{r}{2b} \cos(\theta + \beta) = -\sin \theta \cos \eta \cot 2\eta \dots (21_1)$$

which equals $-\infty$, 0 , $1/2$ for $\eta = 0^\circ$, 45° , 90° . The flow resembles that in Figure 6; it has twin whirls abreast its middle, stop points at $x = \pm a/\sqrt{2}$, and infinite velocity at the edges.

Putting in (1), $r=x$ and $q_0 = -x\Omega_c$ gives the plate's surface pressure

$$p/\frac{1}{2}\rho a^2 \Omega_c^2 = \frac{x^2}{a^2} - \frac{q^2}{a^2 \Omega_c^2} = (1 - \cot^2 2\eta) \cos^2 \eta \dots (22_1)$$

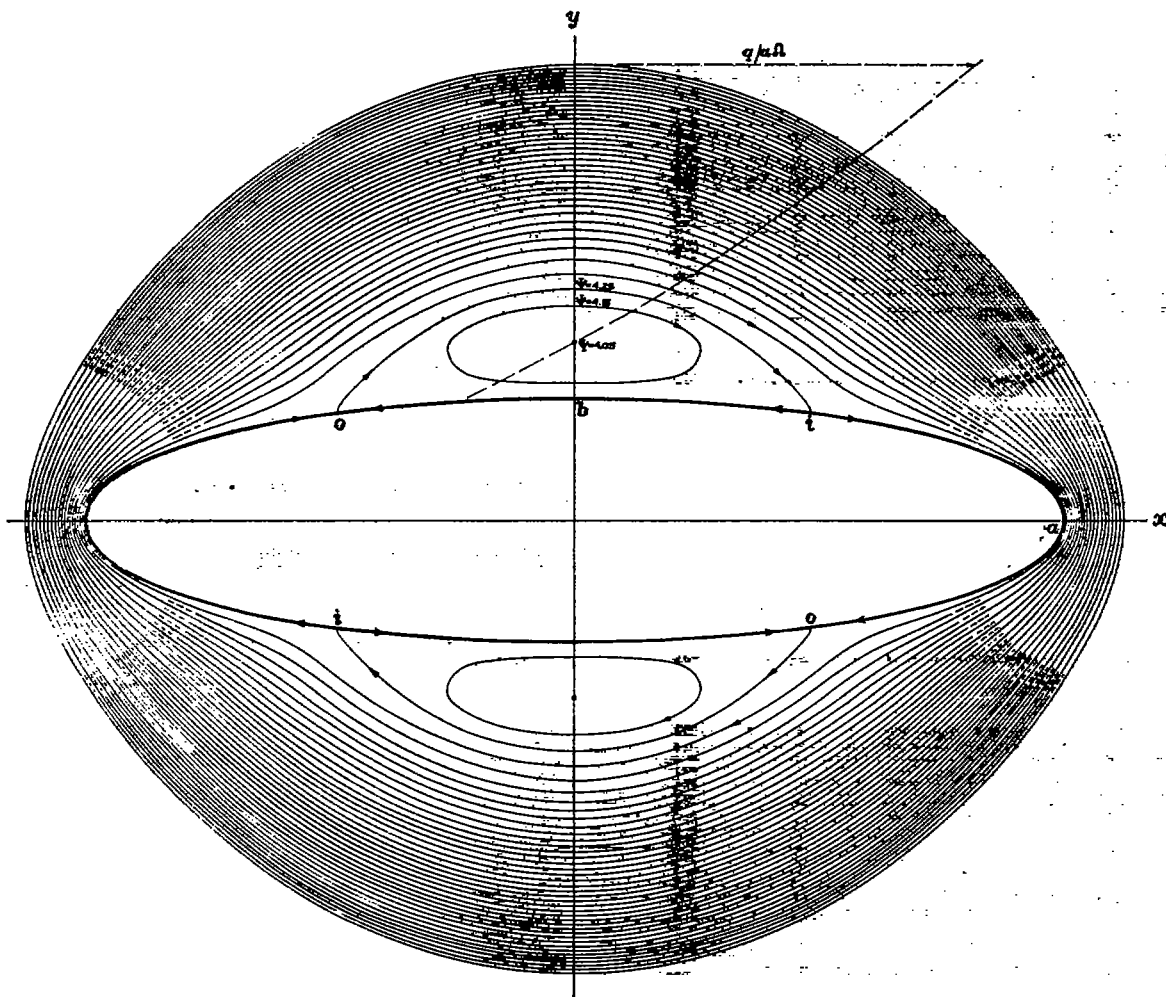


FIGURE 6.—Streamlines about endless elliptic cylinder fixed in infinite inviscid liquid rotating about its long axis with uniform angular speed $-\Omega$; shows $\psi = \frac{1}{2} \Omega (r^2 - m'_c a' b' \cos 2\eta)$ with increments $\Delta \psi = 1$, $\Omega = -1$. Dotted line portrays x -wise speed on y axis

which equals $-1/4$, $1/2$, $-\infty$ for $x=0$, $\pm a/\sqrt{2}$, $\pm a$; viz, for $\eta = 90^\circ$, 45° , 0 , etc.

PROLATE SPHEROID.—For a prolate spheroid, of semiaxes a , b , c , rotating about c with speed Ω_c in an infinite inviscid liquid,

$$\varphi = -m'_c \Omega_c xy = -\frac{1}{2} m'_c \Omega_c a' b' \sin 2\eta \cos \omega \dots (23)$$

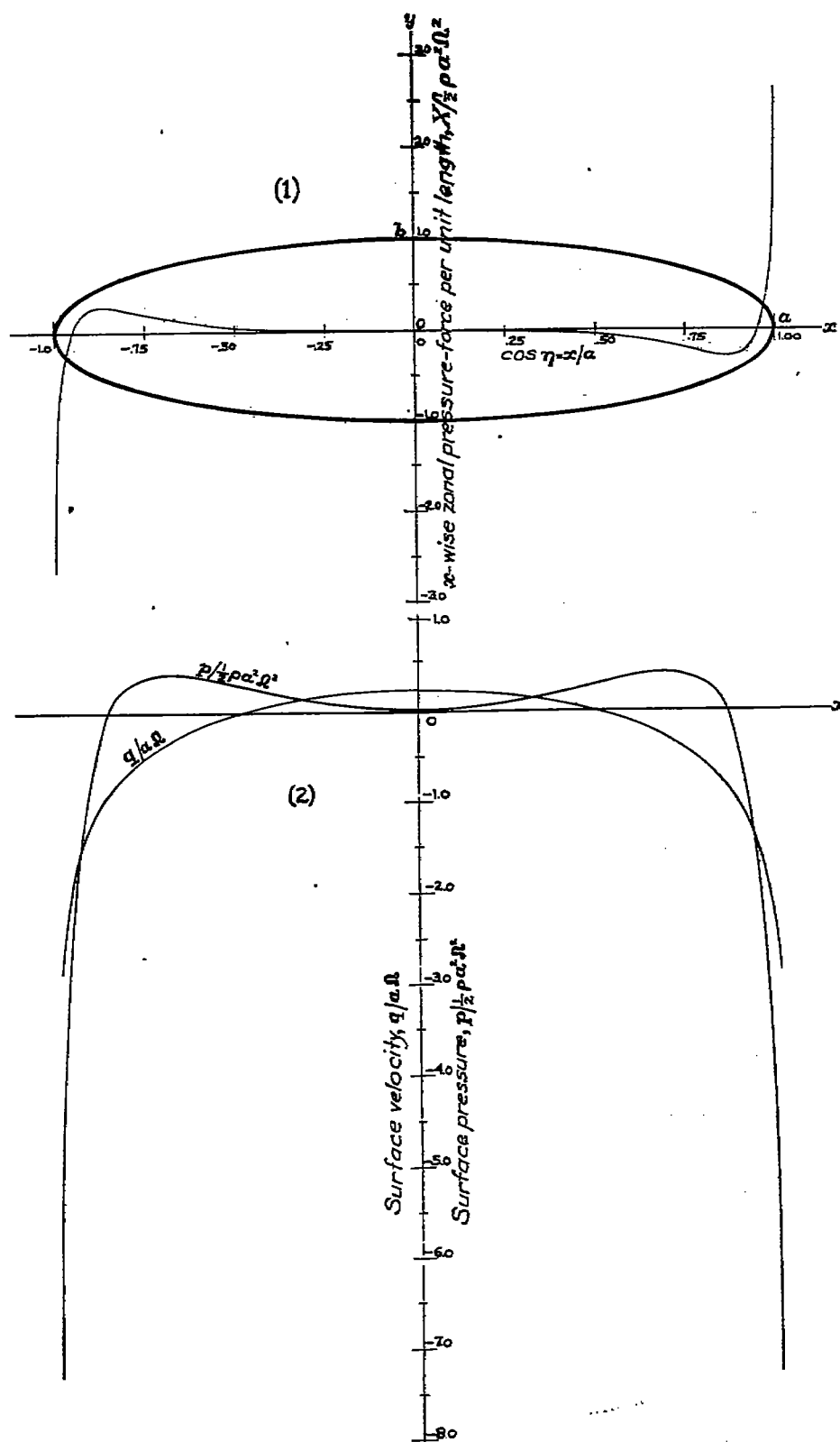


FIGURE 7.—Endless elliptic cylinder fixed in infinite inviscid liquid uniformly rotating about it; shows (1) x -wise zonal pressure-force, $X/2 \rho a^2 \Omega^2$; (2) surface velocity $q/a \Omega$ and surface pressure, $p/2 \rho a^2 \Omega^2$, above or below undisturbed local pressure in uniform stream, $-\Omega$

the geometric symbols being as in Figure 3. For any outer confocal spheroid $a'b'c'$ (23) has the known constant potential coefficient

$$m'_c = \frac{\frac{3}{2e'} \log \frac{1+e'}{1-e'} - 3 - \frac{e'^2}{1-e'^2}}{\frac{3}{2e} (2-e^2) \log \frac{1+e}{1-e} - 6 + \frac{e^2}{1-e^2}} ee' \quad (24)$$

e, e' being the eccentricities of $ab, a'b'$. Table IV gives surface values of m'_c for various shapes of prolate spheroid.

In the yz, zx planes $\varphi=0$; in the xy plane, where $\cos \omega=1$

$$\varphi = -\frac{1}{2} m'_c \Omega_c a' b' \sin 2\eta \quad \psi = -\frac{1}{2} m'_c \Omega_c a' b' \cos 2\eta \quad (23_1)$$

which, except for m'_c , have the same values as (15), entailing the same polar streamlines (18). The equipotentials on $a'b'c'$ are its intersections with the family $xy = -\varphi/m'_c \Omega_c = \text{const.}$

At any point (x, y, z) on $a'b'c'$ the orthogonal velocity components are by (23)

$$q'_n = \frac{\partial \varphi}{\partial e'} \frac{de'}{dn} \quad q'_\eta = \frac{\partial \varphi}{\partial \eta} \frac{d\eta}{ds_\eta} \quad q'_\omega = \frac{\partial \varphi}{\partial \omega} \frac{d\omega}{ds_\omega} \quad (25)$$

$\delta n, \delta s_\eta, \delta s_\omega$ denoting line elements along the normal, meridian, and circle of latitude, as in Figure 3. Since q'_n is absent from (1), we shall not need it; we merely note that on the model's surface it is $r \Omega_c \sin (\theta - \beta) \cos \omega$. By geometry $d\eta/ds_\eta = r \cos (\theta + \beta)/a'b' \cos 2\eta$,⁴ $d\omega/ds_\omega = 1/b' \sin \eta$; hence

$$q'_\eta = -m'_c \Omega_c r \cos (\theta + \beta) \cos \omega \quad q'_\omega = m'_c \Omega_c r \cos \beta \sin \omega \quad (25_1)$$

For $\omega=0$, $q'_\omega (=q'_\eta)$ differs only by m'_c from (17₁) for an elliptic cylinder; also $r \cos \beta = x \therefore q'_\omega = m'_c x \Omega_c \sin \omega=0$, $m'_c x \Omega_c$ for $\omega=0, \pi/2$.

Superposing $-\Omega_c$ on the above system adds to (25₁), as easily appears

$$q''_n = -\Omega_c r \sin (\theta - \beta) \cos \omega \quad q''_\eta = -\Omega_c r \cos (\theta - \beta) \cos \omega \quad q''_\omega = \Omega_c r \cos \beta \sin \omega \quad (26)$$

At the now fixed surface and on the x, y axes $q_n=0=q'_n+q''_n$; hence summing (25₁), (26) gives there

$$\left. \begin{aligned} q_\eta &= -[m'_c \cos (\theta + \beta) + \cos (\theta - \beta)] \Omega_c r \cos \omega \equiv \bar{q}_\eta \cos \omega \\ q_\omega &= (1 + m'_c) \Omega_c r \cos \beta \sin \omega \equiv \bar{q}_\omega \sin \omega \end{aligned} \right\} \quad (27)$$

Thus for $\omega=0$ clearly $q/q_0 = m'_c \cos (\theta + \beta) + \cos (\theta - \beta)$, differing from (21) only by m'_c ; for $\omega=\pi/2$, $q/q_0 = -(1 + m'_c)$, a formula like that for a negative flow q_0 across a cylinder; for $\omega=0^\circ, 90^\circ, 45^\circ$, $q = \bar{q}_\eta, \bar{q}_\omega, \sqrt{\frac{1}{2}(\bar{q}_\eta^2 + \bar{q}_\omega^2)}$. On the x axis $q/q_0 = 1 + m'_c$; on the y axis $q/q_0 = 1 - m'_c > 0$ everywhere, hence no whirl centers on y .

Figure 8 shows $|q/a\Omega_c|$ on the meridians $\omega=0, \pm 45^\circ, \pm 90^\circ$ of a fixed spheroid with $a/b=4$. Distributions symmetrical with these occur on the opposite half of the surface. Noteworthy is q for $\omega=\pm 90^\circ$. By (27) it is $q = \pm (1 + m'_c) \Omega_c x$; hence the straight-line graph in Figure 8.

Figure 8 shows also, for these meridians, the pressure computed with the working formula, derived from (1), (27).

$$\frac{p}{\frac{1}{2} \rho a^2 \Omega_c^2} = A \cos^2 \omega + B \sin^2 \omega \quad (28)$$

⁴ E. g., by (23) $\frac{d}{ds_\eta} xy = \frac{d}{ds_\eta} \left(\frac{1}{2} a'b' \sin 2\eta \cos \omega \right)$; viz, $r \cos (\theta + \beta) = a'b' \cos 2\eta \frac{d\eta}{ds_\eta}$, which gives $\frac{d\eta}{ds_\eta}$ in (25). Also directly $q'_\eta = \frac{\partial \varphi}{\partial \eta} = -m'_c \Omega_c \frac{d}{ds_\eta} xy = -m'_c \Omega_c r \cos (\theta + \beta) \cos \omega$.

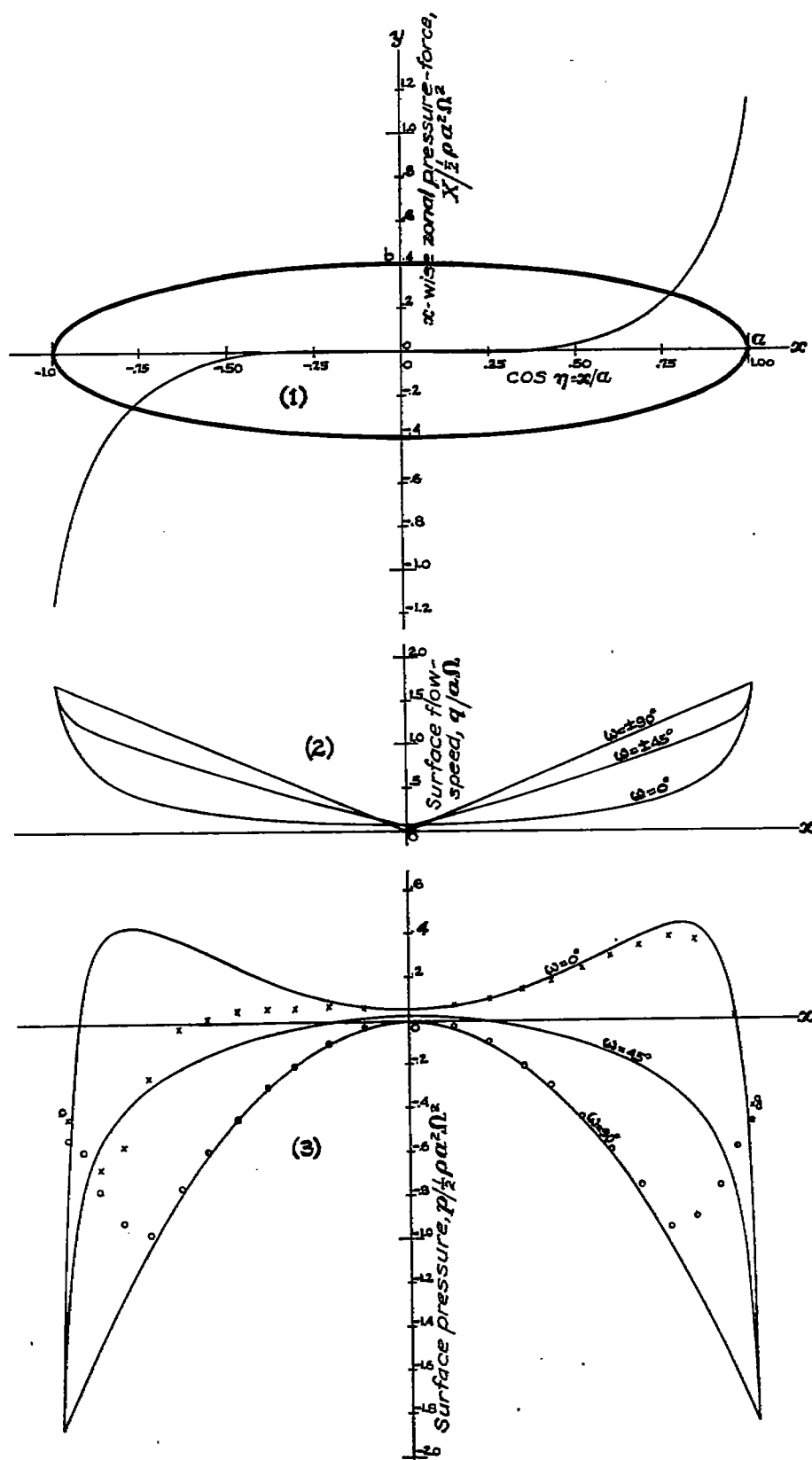


FIGURE 8.—Prolate spheroid fixed in infinite inviscid liquid uniformly rotating about it; shows (1) x -wise zonal pressure-force, $X/\frac{1}{2}\rho a^2\Omega^2$; (2) surface flow-speed, $q/a\Omega$; (3) surface pressure, $p/\frac{1}{2}\rho a^2\Omega^2$, above or below undisturbed local pressure in uniform stream, $-\Omega$. Crosses and circles give measured air pressures for $\Omega = -39.5$ radians per second given in reference 3

where $A = (1 - [m'_c \cos(\theta + \beta) + \cos(\theta - \beta)]^2) \cos^2 \eta / \cos^2 \beta$, $B = -m'_c(2 + m'_c) \cos^2 \eta$. Here $m'_c = .689$ by Table IV. The crosses and circles, giving experimental values taken from Reference 3, show good agreement with (28) for a considerable part of the surface. For $\cos \omega = 0$, $p \propto B \propto x^2$; or the graph is parabolic.

Integrating p , as in (9), (10), gives for an inviscid liquid $Y = 0 = N$, $X \neq 0$. Figure 8 portrays X computed from theory and experiment.

ELLIPSOID.—For an ellipsoid, of semiaxes a, b, c along x, y, z , rotating about c with speed Ω_c in an infinite inviscid liquid, otherwise still,

$$\varphi = -m'_c \Omega_c xy \quad (29)$$

which for any outer confocal ellipsoid $a'b'c'$, has the constant potential coefficient

$$m'_c = C(\beta - \alpha) \quad C = \frac{a^2 - b^2}{2(a^2 - b^2) - (a^2 + b^2)(\beta_0 - \alpha_0)} \quad (30)$$

the Greek letters being as in Part V. Surface values of m'_c are listed in Table IV.

By (29) the equipotential lines on $a'b'c'$ are its intersections with the hyperbolic cylinder family $xy = -\varphi/m'_c \Omega_c = \text{const.}$ The orthogonals to $\varphi = \text{const.}$ at the surface $a'b'c'$ are the streamlines there. These by (31) are parallel to x where $x=0$; parallel to y where $y=0$; normal to z where $z=0$. The same obviously holds for spheroids and other ellipsoidal forms.

In the xy plane the flow has the polar streamlines (18); also it has there

$$\varphi = -\frac{1}{2} m'_c \Omega_c a' b' \sin 2\eta \quad \psi = -\frac{1}{2} m'_c \Omega_c a' b' \cos 2\eta \quad (29_1)$$

whence the streamlines in that plane are plotted. The form of (29₁) is like those of (15) and (23₁), for the elliptic cylinder and prolate spheroid, entailing similar expressions for the velocity and pressure in the plane-flow field $z=0$.

For the general flow the velocity components at $a'b'c'$ are by (29)

$$u' = -\left(x \frac{\partial m'_c}{\partial x} + m'_c\right) \Omega_c y \quad v' = -\left(y \frac{\partial m'_c}{\partial y} + m'_c\right) \Omega_c x \quad w' = -\Omega_c xy \frac{\partial m'_c}{\partial z} \quad (31)$$

and those due to the superposed velocity $-\Omega_c R = q_0$, are

$$u'' = \Omega_c y \quad v'' = -\Omega_c x \quad w'' = 0 \quad (32)$$

whence the resultant velocity and pressure may be derived for all points of the flow field about the ellipsoid fixed in the steady stream $-\Omega_c R$. In forming the x, y, z derivatives of m'_c one may use the relations (14) and (72).

Everywhere in the planes $x=0, y=0$, the resultant velocities are, respectively, by (31) and (32),

$$q = u = (1 - m'_c) \Omega_c y \quad q = v = -(1 + m'_c) \Omega_c x \quad (33)$$

while in the plane $z=0$, q can be found as indicated for an elliptic cylinder. (33) apply also to the elliptic cylinder and prolate spheroid previously treated, and to all other forms of the ellipsoid fixed in the flow $-\Omega_c$.

(B) BODIES IN COMBINED TRANSLATION AND ROTATION

MOST GENERAL MOTION.—The most general motion of any body through a fluid may have the components U, V, W along, and $\Omega_a, \Omega_b, \Omega_c$ about, three axes, say a, b, c . The entailed resultant particle velocity q' at any flow point is found by compounding there the individual velocities severally due to $U, V, W, \Omega_a, \Omega_b, \Omega_c$, and computable for an ellipsoid by formulas in Reference 2 and the foregoing text.

YAWING FLIGHT.—In airship study the flow velocity q' caused by a prolate spheroid in steady circular flight is specially interesting. Let the spheroid's center describe about 0,

Figure 9, a circle of radius na , with path speed $na\Omega$. Then if α is the constant yaw angle of attack, the component centroid velocities along a , b , and the steady angular speed about c are, respectively,

$$U = na\Omega \cos \alpha \quad V = na\Omega \sin \alpha \quad \Omega_c = \Omega \quad (34)$$

If, now, velocities the reverse of (34) are imposed on the body and fluid, $q_s = 0$, and the surface velocity q on the fixed spheroid has in longitude and latitude the respective components

$$\left. \begin{aligned} q_\theta &= (1+k_s)U \sin \theta - (1+k_b)V \cos \theta \cos \omega - [m'_c \cos (\theta + \beta) + \cos (\theta - \beta)]\Omega_c r \cos \omega \\ q_\omega &= (1+k_s)V \sin \omega + (1+m'_c)\Omega_c r \cos \beta \sin \omega \end{aligned} \right\} \quad (35)$$

where positive flows along ds are, respectively, in the directions of increasing η , ω , as in Figure 3. The terms in U , V , are known formulas for translational flow, e. g., Reference 2; the others are from (27). Hence q^2 then p is found for any point (β, ω) on the spheroid.⁵ If Ω_c is negligible, $q = \bar{q} \sin \epsilon$, where $\bar{q}^2 = (1+k_s)^2 U^2 + (1+k_b)^2 V^2$, and ϵ is the angle between the local and polar normals, as proved in Reference 2.

Figure 9₂ portrays, for specified conditions, theoretical values of $p/\frac{1}{2}\rho Q^2$, Q being the path speed $\sqrt{U^2 + V^2}$ of the spheroid's center; it also portrays $p/\frac{1}{2}\rho Q^2$ for the model in rectilinear motion, with $Q = U$. The difference of $p/\frac{1}{2}\rho Q^2$ for straight and curved paths, though material, is less than experiment gives, as shown by 9₃. Fuller treatment and data are given in Reference 3.

The forces X , Y and moment N , for any zone, may be computed as before; but for the whole model they are more readily found by the method of Part IV. Zonal Y and N for a hull form are found in Part III.

The first of (35) applies also to an elliptic cylinder, with $\cos \omega = 1$, $m'_c = (a^2 - b^2)/2ab$. Fixed in a flow $-U$, $-V$, $-\Omega_c$, it has the surface velocity

$$q = (1+b/a)U \sin \theta - (1+a/b)V \cos \theta - \left[\frac{a^2 - b^2}{2ab} \cos (\theta + \beta) + \cos (\theta - \beta) \right] \Omega_c r \quad (36)$$

For an endless flat plate $b = 0$, $\cos \theta = b/a \sin \theta \cot \eta$; and the last term of (36) may be rewritten by (21₁); thus (36) becomes

$$q = (U - V \cot \eta - a\Omega_c \cos \eta \cot 2\eta) \sin \theta \quad (37)$$

These two values of q with (1₁) give the pressure distribution over an elliptic cylinder or flat plate revolving about an axis parallel to its length or fixed in a fluid rotating about that axis.

Thus an endless plate of width $2a$, revolving with angular speed Ω , path radius na , and incidence α , as in Figure 10₁, has by (37) the relative surface velocity, viz, slip velocity

$$q/a\Omega = (n \cos \alpha - n \sin \alpha \cot \eta - \cos \eta \cot 2\eta) \sin \theta \quad (38)$$

and since $\sin^2 \theta = 1$, $q_0^2 = U^2 + (V + x\Omega)^2 = a^2 \Omega^2 (n^2 + 2n \sin \alpha \cos \eta + \cos^2 \eta)$, (1) gives

$$p/\frac{1}{2}\rho a^2 \Omega^2 = \eta^2 + 2n \sin \alpha \cos \eta + \cos^2 \eta - n^2 (\cos \alpha - \sin \alpha \cot \eta - \frac{1}{n} \cos \eta \cot 2\eta)^2 \quad (39)$$

For $n = 3$, $\alpha = 30^\circ$, Figure 10₂ delineates the distribution of slip velocity $q/a\Omega$ on both sides of the plate; 10₃ that of the pressure $p/\frac{1}{2}\rho a^2 \Omega^2$ on its two faces. This pressure integrated over the plate's double surface gives $F = 0$, as may be shown. The dashed line in Figure 10₃ is the pressure-difference graph whose integral for $\eta = 0$ to π is also zero. The resultant forces X , Y and moment N for such a plate are found in Part IV by a method simpler than surface integration of the pressure.

⁵ Here again q is the slip speed of the flow at any point of the body's surface, and depends only on the relative motion of body and fluid.

FLOW INSIDE ELLIPSOID.—At any point inside an ellipsoid with speeds U , V , W , Ω_a , Ω_b , Ω_c , along and about a , b , c , filled with inviscid liquid otherwise still,

$$\varphi = Ux + Vy + Wz + \frac{b^2 - c^2}{b^2 + c^2} \Omega_a yz + \frac{c^2 - a^2}{c^2 + a^2} \Omega_b zx + \frac{a^2 - b^2}{a^2 + b^2} \Omega_c xy \quad (40)$$

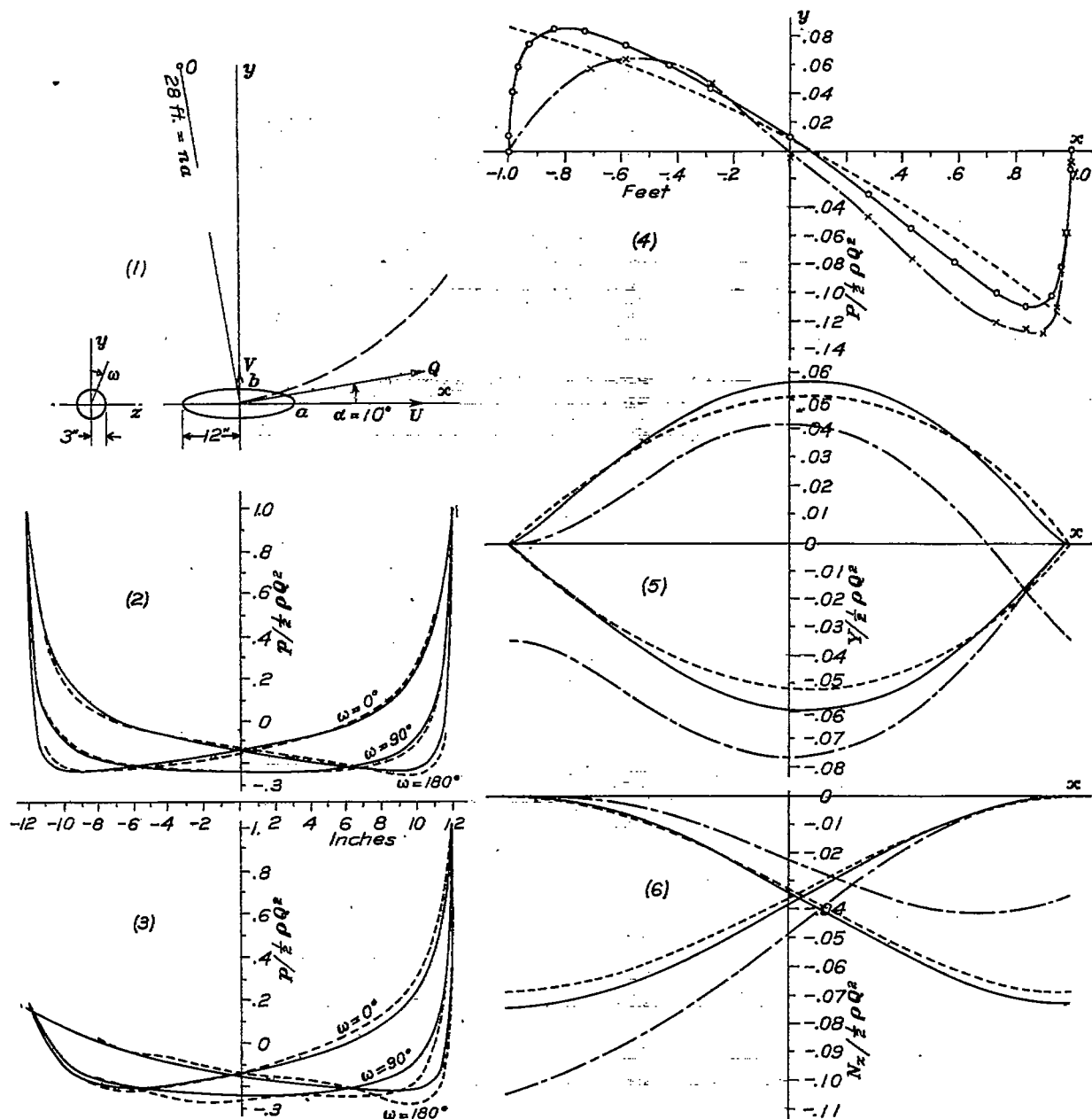


FIGURE 9.—Prolate spheroid in steady yawing flight. (1) Defines velocity conditions; (2) delineates theoretical pressure distribution; (3) experimental pressure distribution for $Q=40$ feet per second. In (2) and (3), full lines indicate rectilinear, dashed lines curvilinear motion

FIGURE 9 (continued).—For conditions (1), (4) delineates pressure load per unit length; (5) the zonal force; (6) the zonal moment. In (4) the full and dotted lines give theoretical values from equations (a), (b); the dashed line, experimental values from reference 3. (5) is obtained by planimetry (4); (6) by planimetry (5)

whose coefficients are constant for the whole interior. Hence the components of the particle velocity q are

$$\frac{\partial \varphi}{\partial x} = u = U + \frac{c^2 - a^2}{c^2 + a^2} \Omega_b z + \frac{a^2 - b^2}{a^2 + b^2} \Omega_c y \quad (41)$$

and like values for v , w found by permuting the symbols. If the fluid were solidified any particle would have

$$u = U + \Omega_b z - \Omega_c y, \text{ etc., etc.} \quad (42)$$

Thus when an ellipsoid full of inviscid still fluid is given any pure translation its content moves as a solid; but when given pure rotation each particle moves with less speed than if the fluid were solidified, since the fractions in (41) are less than unity.

For velocities U , V , Ω_c of the ellipsoid

$$\varphi = Ux + Vy + \frac{a^2 - b^2}{a^2 + b^2} \Omega_c xy \quad (43)$$

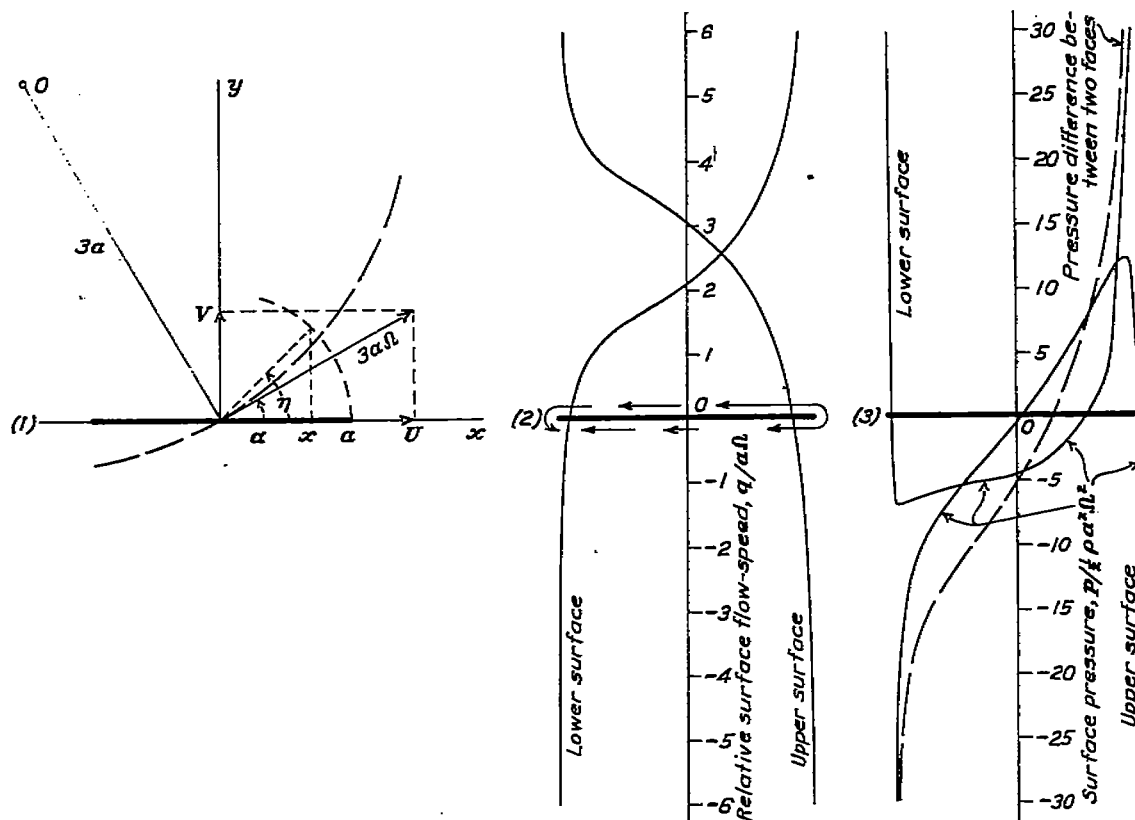


FIGURE 10.—Endless flat plate revolving about axis parallel to its length, in infinite inviscid fluid. (1) Defines conditions; (2) delineates relative velocity $q/a \Omega$ of fluid; (3) pressure $p/\frac{1}{2} \rho a^2 \Omega^2$, and pressure difference $\Delta p/\frac{1}{2} \rho a^2 \Omega^2$ on two faces of plate

for which $w = \partial \varphi / \partial z = 0$. For this plane flow (4) with (43) gives

$$\psi = Uy - Vx - \frac{1}{2} \Omega_c \frac{a^2 - b^2}{a^2 + b^2} (x^2 - y^2) \quad (44)$$

whence the streamlines may be plotted. In particular if the model has simple rotation Ω_c ,

$$x^2 - y^2 = -2 \frac{a^2 + b^2}{a^2 - b^2} \psi / \Omega_c = \text{const.} \quad (45)$$

and the interior streamlines are hyperbolas, as in Figure 5.

Adding (2) to ψ in (45) gives the steady flow

$$\psi = \frac{\Omega_c}{a^2 + b^2} (a^2 y^2 + b^2 x^2) \quad (46)$$

hence the streamlines lie on the elliptic cylinders

$$a^2 y^2 + b^2 x^2 = (a^2 + b^2) / \Omega_c \psi = \text{const.} \quad (47)$$

By (46) $q = 2\Omega_c(a^2y^2 + b^2x^2)^{1/2}/(a^2 + b^2)$, which put in (1) gives at (x, y) , since $q_0 = -\Omega_c R$,

$$p_n - p = \frac{4(a^2y^2 + b^2x^2)}{(a^2 + b^2)^2(x^2 + y^2)} p_n \quad (48)$$

where $p_n = \rho q_0^2/2$. Here p_n is the centrifugal pressure due to the fluid's peripheral velocity q_0 , and p is the pressure change due to $q_0 - q$, q being the relative velocity of fluid and container. In a like balloon hull q would quickly damp out, leaving only p_n as the dynamic pressure. At the ends of a, b, c , respectively, (48) gives

$$\frac{p_n - p}{p_n} = \frac{4b^4}{(a^2 + b^2)^2} - \frac{4a^4}{(a^2 + b^2)^2} \approx 0.$$

For large a/b the first is negligible, the second approaches 4, giving $p = -3p_n = -1.5\rho\Omega_c^2 b^2$ as the temporary dynamic pressure drop inside the hull at the end of b . Experimental proof would be interesting.

POTENTIAL COEFFICIENTS.—An ellipsoid of semiaxes a, b, c along x, y, z , when moving through an infinite inviscid liquid, otherwise still, with velocities $U, V, W, \Omega_a, \Omega_b, \Omega_c$ along and about the instantaneous lines of a, b, c , begets the known velocity potential

$$\varphi = -m_a Ux - m_b Vy - m_c Wz - m'_a \Omega_a yz - m'_b \Omega_b zx - m'_c \Omega_c xy \quad (49)$$

the six potential coefficients m being constant over any outer confocal ellipsoid $a'b'c'$. Their values for abc are given in Tables III, IV. Alternatively (49) can be written for this surface

$$\varphi = -k_a Ux - k_b Vy - k_c Wz - \frac{b^2 + c^2}{b^2 - c^2} k'_a \Omega_a yz - \frac{c^2 + a^2}{c^2 - a^2} k'_b \Omega_b zx - \frac{a^2 + b^2}{a^2 - b^2} k'_c \Omega_c xy \quad (50)$$

the k s being the more familiar inertia coefficients defined and tabulated in Part V. Of the six potential coefficients in (50) the first three are the same as the inertia coefficients k_a, k_b, k_c ; the last three are greater except when c/b or a/c or b/a is zero. Thus, if $b/a = 0$ the last term of (50) is $-k'_c \Omega_c xy$, which is the potential on the outer surface of an elliptic cylinder ($a = \infty$) rotating about c . Everywhere inside of it the potential is $\Omega_c xy$, as (40) shows.

For the flow (40) textbooks give the inertia coefficients

$$k_a, k_b, k_c = 1 \quad k'_a = \left(\frac{b^2 - c^2}{b^2 + c^2}\right)^2 \quad k'_b = \left(\frac{c^2 - a^2}{c^2 + a^2}\right)^2, \text{ etc.} \quad (51)$$

which are the squares of the potential coefficients. One notes too that the ratios of like terms in (40), (50) equal the ratios of like potential coefficients and like inertia coefficients, which latter in turn are known to equal the ratios of like kinetic energies of the whole outer and inner fluids, if the inner moves as a solid.

RELATIVE VELOCITY AND KINETIC PRESSURE.—When a body moves steadily through a perfect fluid, otherwise still, the absolute flow velocity it begets at any point (x, y, z) , being unsteady, is not a measure of the pressure change there. The relative velocity is such a measure. To find it we superposed on the moving body and its flow field an equal counter velocity, thus reducing the body to rest and making the flow about it steady. The same result would follow from geometrically adding to said absolute flow velocity the reversed velocity of (x, y, z) assumed fixed to the body. In particular this process gives for any point of the body's surface the wash velocity, or slip speed, which with Bernoulli's principle determines the entailed change of surface pressure. Conversely, if the pressure change at a point is known or measured, it determines the relative velocity there. In hydrodynamic books the above reversal is used commonly enough for bodies in translation. In this text it is employed as well for rotation; also for combined translation and rotation. However general its steady motion, the body is steadily accompanied by a flow pattern whose every point, fixed relatively to the body, has constant relative velocity and constant magnitude of instantaneous absolute velocity and pressure.

REPORT No. 323

FLOW AND FORCE EQUATIONS FOR A BODY REVOLVING IN A FLUID

PART III

ZONAL FORCES ON HULL FORMS¹

PRESSURE LOADING.—For a prolate spheroid abc with speeds U , V , Ω_c , Figure 9₁, or fixed in a stream $-U$, $-V$, $-\Omega_c$, (35) gives at (x, y, z) on abc the relative velocity

$$q^2 = q_{\eta}^2 + q_{\omega}^2 = A - B \cos \omega + C \cos^2 \omega$$

A , B , C being constant for any latitude circle. In forming this equation one finds

$$B = 2(1 + k_a)U \sin \theta \{ (1 + k_b)V \cos \theta + [m'_c \cos (\theta + \beta) + \cos (\theta - \beta)]r\Omega_c \},$$

etc., for A , C . In the body's absence said stream has, at said point (x, y, z) ,

$$q_0^2 = (-U + y\Omega_c)^2 + (-V - x\Omega_c)^2 = A_1 - B_1 \cos \omega + C_1 \cos^2 \omega,$$

where ω alone varies on the latitude circle. Its radius being $y_0 = z_0$, makes $y = y_0 \cos \omega$,

$$B_1 = 2Uz_0\Omega_c,$$

etc., for A_1 , C_1 . Putting q , q_0 in (1) gives the surface pressure

$$p/.5\rho = q_0^2 - q^2 = (A_1 - A) + (B - B_1) \cos \omega + (C_1 - C) \cos^2 \omega.$$

By (10₁) the loading per unit length of x is, since $\int_0^{2\pi} \cos \omega d\omega = 0 = \int_0^{2\pi} \cos^3 \omega d\omega$,

$$P/.5\rho = -\frac{z_0}{.5\rho} \int_0^{2\pi} p \cos \omega d\omega = -(B - B_1)z_0 \int_0^{2\pi} \cos^2 \omega d\omega = -\pi(B - B_1)z_0 \dots \dots \dots (a)$$

A , A_1 , C , C_1 vanishing on integration of p . Thus, finally,

$$P/.5\rho Q^2 = -\pi(B - B_1)z_0/Q^2 \dots \dots \dots (a_1)$$

P having the direction of the cross-hull component of p at $\omega = 0$.

One notes that $q_{\omega}^2 (\propto \sin^2 \omega)$ contributes nothing to B or the integral in (a); viz, the loading P is unaffected by q_{ω} , and depends solely on q_{η} , the meridian component of the wash velocity. Also for $\beta = 0$ and π , $B - B_1 = 0 = P$.

In Figure 9₄ the full line depicts (a₁) for the spheroid shown in 9₁, circling steadily at 40 feet per second. The theoretical dots closely agreeing with it are from Jones, Reference 3, as is also the experimental graph. Beside them is a second theoretical graph plotted from Doctor Munk's approximate formula derived in Reference 8 and given in the next paragraph. But that Professor Jones omitted some minor terms in his value of p , his theoretical $P/.5\rho Q^2$ should exactly equal (a₁). His formula, derived by use of Kelvin's $p_0/\rho = \dot{\phi} - q^2/2$, can best be studied in the detailed treatment of Reference 3.

In Reference 8 Professor Ames derives Munk's airship hull formula

$$\frac{P}{.5\rho Q^2} = \sin 2\alpha \frac{dS}{dx} + \frac{2}{R} \frac{d}{dx} (xS),$$

¹ This part was added after Parts I, II, IV, V were typed; hence the special numbering of the equations.

S being the area of a cross-section; R the radius of the path of the ship's center. This was assumed valid for a quite longish solid of revolution; for a short one it was hypothetically changed to

$$\frac{P}{.5\rho Q^2} = (k_b - k_a) \sin 2\alpha \frac{dS}{dx} + 2 \frac{k'_e}{R} \frac{d}{dx} (xS) \quad (b)$$

Applying this to a prolate spheroid we derive the working formula

$$\frac{P}{.5\rho Q^2} = -Lx - Mx^2 + N \quad (b_1)$$

where the constants for a fixed angle of attack are²

$$L = 2(k_b - k_a) \frac{b^2}{a^2} \cdot \pi \sin 2\alpha, \quad M = 3k'_e \frac{b^2}{a^2} \cdot \frac{2\pi}{R} \cos \alpha, \quad N = k'_e b^2 \cdot \frac{2\pi}{R} \cos \alpha.$$

Plotting (b₁) for the conditions in 9₁ gives the dotted curve in 9₄. It shows large values of $P/.5\rho Q^2$ for the ends of the spheroid, where (a₁) gives zero. To that extent it fails, though with little consequent error in the zonal force and moment at the hull extremities. It has the merit of being convenient and applicable to any round hull whose equation may be unknown or difficult to use.

ZONAL FORCE.—An end segment of the prolate spheroid, say beyond the section $x = x_1$, bears the resultant cross pressure

$$Y = \int_{x_1}^a P dx \quad (c)$$

which with the resisting shear at x_1 must balance the cross-hull acceleration force on the segment in yawing flight. For the whole model (b₁) with (c) gives $Y = 0$, which is not strictly true for curvilinear motion; but (a₁) with (c) gives the correct theoretical value of Y , and agrees with (67).

In Figure 9₅ graphs of $Y/.5\rho Q^2$, for the values (a₁) and (b₁) of P , are shown beside those derived from Jones' experimental pressure curve. Since Y is proportional to the area of a segment of the graph of P , it can be found by planimentering the segment or by integrating $P dx$.

ZONAL MOMENT.—The loading P exerts on any end segment, say of length $a - x$, the moment about its base diameter z

$$N_z = \int_x^a Y dx$$

which can be found by planimentering the graph of Y . Figure 9₆ delineates N_z so derived from the three graphs of Y . They show the moment on the right hand segment varying in length from 0 to $2a$; also on the left segment of length from 0 to $2a$. The resisting moment of the cross section must balance N_z and the acceleration moment of the segment.

CORRECTION FACTORS.—No attempt is here made to deduce theoretically a correction factor to reconcile the computed and measured p . In Reference 3 Jones shows that the theoretical and experimental graphs of $P/.5\rho Q^2$ have, for any given latitude $x_1 > a/2$, the same difference of ordinate whatever the incidence $0 < \alpha < 20^\circ$. Thus the ordinate difference found for the zero-incidence graphs, when applied to the theoretical graph for any fixed $0 < \alpha < 20^\circ$, determines the experimental one with good accuracy. Such established agreement in loading favorably affects, in turn, the graphs of Y , N_z , the transverse force and moment on any end segment of the spheroid.

² From the meridian curve $\frac{x^2}{a^2} + \frac{y^2}{b^2} = 1$, $\frac{dy}{dx} = -\frac{b^2}{a^2} \frac{x}{y}$, $S = \pi y^2$; hence $\frac{dS}{dx} = 2\pi y \frac{dy}{dx} = -2\pi \frac{b^2}{a^2} x$, which put in (b) leads to (b₁).

REPORT No. 323

FLOW AND FORCE EQUATIONS FOR A BODY REVOLVING IN A FLUID

PART IV

RESULTANT FORCE AND MOMENT

BODY IN FREE SPACE.—Let a homogeneous ellipsoid of semiaxes a, b, c move freely with component velocities u, v, w, p, q, r ¹ respectively along and about instantaneous fixed space axes x, y, z coinciding at the instant with a, b, c . Then the linear and angular momenta referred to x, y, z are

$$m_1 u \quad m_1 v \quad m_1 w \quad A_1 p \quad B_1 q \quad C_1 r \text{-----} (52)$$

m_1 being the body's mass, A_1, B_1, C_1 its moments of inertia about a, b, c . If, now, forces X_1, Y_1, Z_1 and moments L_1, M_1, N_1 are applied to the body along and about x, y, z , they cause in the vectors (52) the well-known change rates

$$\left. \begin{aligned} m_1(\dot{u} - rv + qw) &= X_1 & A_1\dot{p} - (B_1 - C_1)qr &= L_1 \\ m_1(\dot{v} - pw + ru) &= Y_1 & B_1\dot{q} - (C_1 - A_1)rp &= M_1 \\ m_1(\dot{w} - qu + pv) &= Z_1 & C_1\dot{r} - (A_1 - B_1)pq &= N_1 \end{aligned} \right\} \text{-----} (53)$$

which apply to any homogeneous solid symmetrical about the planes ab, bc, ca .

For motion in the ab plane; viz, for $w, p, q = 0$; (53) give

$$X_1 = m_1(\dot{u} - rv) \quad Y_1 = m_1(\dot{v} + ru) \quad N_1 = C_1\dot{r} \text{-----} (54)$$

and for uniform revolution about an axis parallel to z , as in Figure 11, viz, for $\dot{u}, \dot{v}, \dot{r} = 0$, (54) become

$$X_1 = -m_1 rv \quad Y_1 = m_1 ru \quad N_1 = 0 \text{-----} (55)$$

where now X_1, Y_1 are merely components of the centripetal force $m_1 r \sqrt{u^2 + v^2}$, whose slope is $Y_1/X_1 = -u/v$. Also if $Q = \sqrt{u^2 + v^2}$ is the path velocity of the body's centroid, h its path radius, $r = Q/h$ is the angular velocity of h and of vector $m_1 Q$.

REACTIONS OF FLUID.—If external forces impel the ellipsoid from rest in a quiescent frictionless infinite liquid, with said velocities u, v, w, p, q, r , they beget in the fluid the corresponding linear and angular momenta

$$k_a m u \quad k_b m v \quad k_c m w \quad k'_a A p \quad k'_b B q \quad k'_c C r \text{-----} (56)$$

where m is the mass of the displaced fluid, and A, B, C its moments of inertia about a, b, c .

One calls $k_a m, k_b m, k_c m$ the "apparent additional masses"; $k'_a A, k'_b B, k'_c C$ the "apparent additional moments of inertia," of the body for its axial directions; because the fluid's resistance to its linear and angular acceleration gives the appearance of such added inertia in the body. The six k 's are called "inertia coefficients," and are shape constants. Values of them are given in Tables III, VI, VIII for various simple quadrics.

The component flow momenta (56), like (52), are vectors along the instantaneous directions of a, b, c ; viz, along x, y, z ; hence their time rates of change must equal the forces and moments which the body exerts on the fluid; viz,

$$\left. \begin{aligned} X &= m(k_a \dot{u} - k_b rv + k_c qw) & L &= k'_a A \dot{p} - (k'_b B - k'_c C)qr - (k_b - k_c)m v w \\ Y &= m(k_b \dot{v} - k_c pw + k_a ru) & M &= k'_b B \dot{q} - (k'_c C - k'_a A)rp - (k_c - k_a)m w u \\ Z &= m(k_c \dot{w} - k_a qu + k_b pv) & N &= k'_c C \dot{r} - (k'_a A - k'_b B)pq - (k_a - k_b)m u v \end{aligned} \right\} \text{----} (57)$$

¹ These new meanings of u, v, w, p, q, r are assigned for convention's sake and for convenience.

all written from (53) on replacing its momenta by those of (56), and adding vector-shift terms. Thus the vector $k_c m v$ shifts with speed v entailing the change rate $k_c m v \cdot v$ of angular momentum about x , while $k_b m v$ shifts with speed w entailing the opposite rate $-k_b m v \cdot w$. Their sum is $(k_c - k_b) m v w$. Permuting these gives for the y, z axes $(k_a - k_c) m w u$, $(k_b - k_a) m u v$. When the k 's are equal the vector-shift terms vanish, as for said free body, or for a sphere, cube, etc., in a fluid. The fluid reactions are (57) reversed. (57) apply also to fluid inside the trisymmetrical surface.

If the angle of attack is $\alpha = \tan^{-1} v/u$, we may write in (53), (57)

$$r = Q/h \quad u = Q \cos \alpha \quad v = Q \sin \alpha \quad uv = \frac{1}{2} Q^2 \sin 2\alpha \quad (58)$$

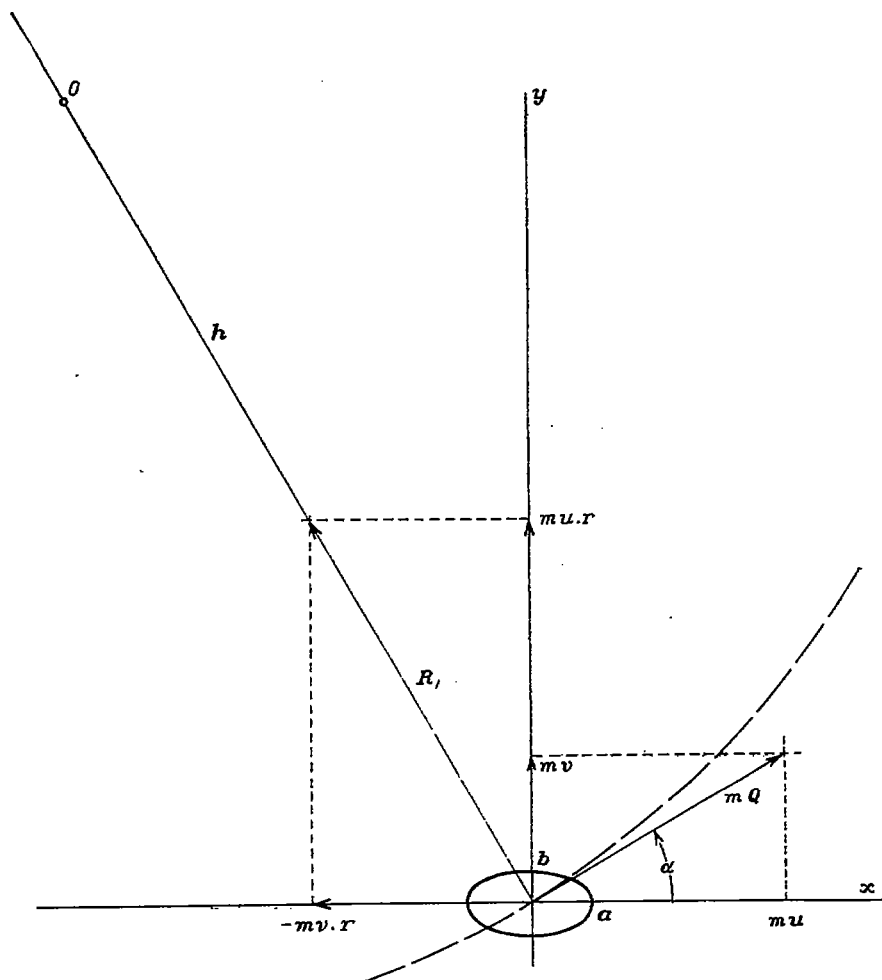


FIGURE 11.—Momenta and forces for free body in uniform circular motion. Centripetal force, $R_1 = mQr = mQ^2/h$, has slope $-u/v$, r being angular speed about 0

Of special aeronautic interest are (57) for plane motion, such as in yawing airship flight, for which $w, p, q = 0$, giving

$$X = m(k_a \dot{u} - k_b r v) \quad Y = m(k_b \dot{v} + k_a r u) \quad N = k'_c C \dot{r} + (k_b - k_a) m u v \quad (59)$$

Thus for uniform circular flight

$$X = -k_b m r v \quad Y = k_a m r u \quad N = (k_b - k_a) m u v \quad (60)$$

which are the analogues of (55) for the free body. Or in notation (58)

$$X = -\frac{k_b \tau}{h} \rho Q^2 \sin \alpha \quad Y = \frac{k_a \tau}{h} \rho Q^2 \cos \alpha \quad N = (k_b - k_a) \tau \frac{\rho Q^2}{2} \sin 2\alpha \quad (61)$$

τ being the volume of the model.

As shown in Figure 12 (60) give the resultant force and slope

$$R^2 = mr \sqrt{k_a^2 u^2 + k_b^2 v^2} \quad Y/X = -\frac{k_a}{k_b} \cot \alpha = -\cot \beta \quad (62)$$

also R and N at the origin are equivalent to a parallel force R through the path center O , along a line (called the central axis of the force system) whose arm and intercepts are

$$l = N/R = h \sin (\beta - \alpha) \quad x = l \sec \beta \quad y = l \operatorname{cosec} \beta \quad (63)$$

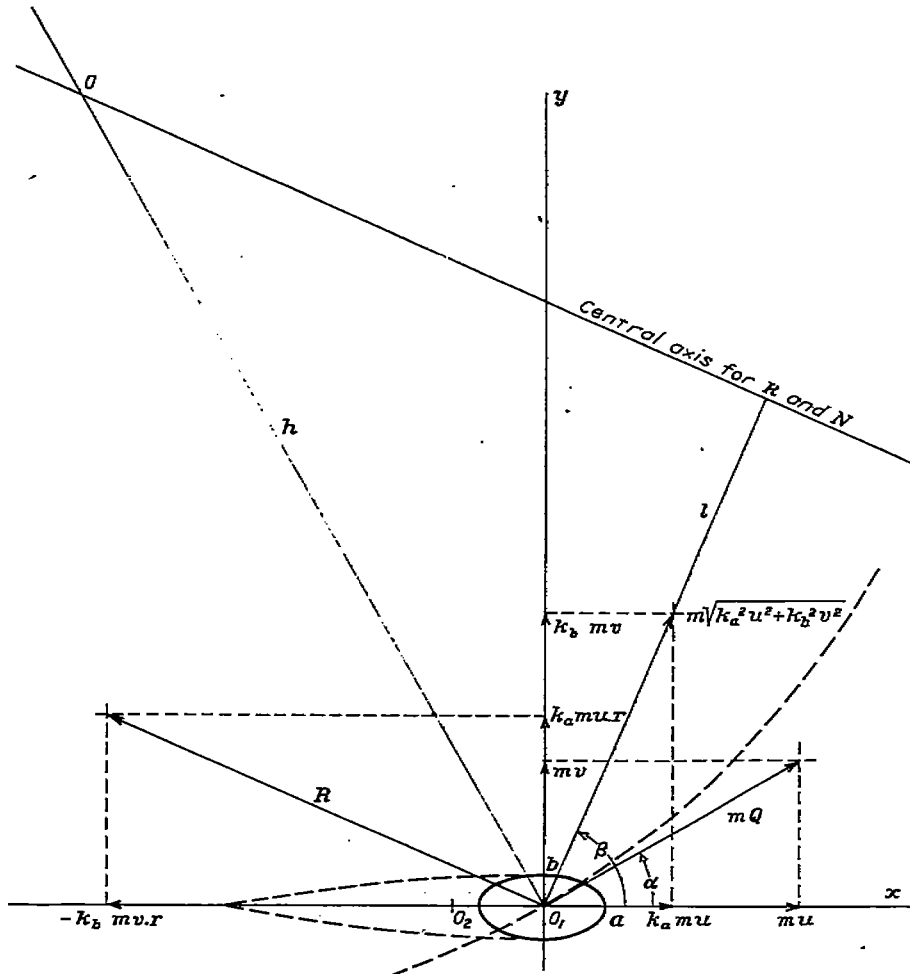


FIGURE 12.—Moments and forces for symmetrical body in uniform circular motion through frictionless infinite liquid otherwise at rest. Whole hydrodynamic force, $R = mr \sqrt{k_a^2 u^2 + k_b^2 v^2}$, has slope $-k_a u/k_b v$. Yaw moment $N = (k_b - k_a) m u v = (k_b - k_a) \tau \frac{\rho Q^2}{2} \sin 2\alpha$, τ being volume

For steady motion (60) show that the body sustains no force in pure translation ($r=0$); no force nor moment in pure rotation ($u, v=0$); no moment in revolution about a point on x or y ; viz, for $u=0$, or $v=0$. For given u, v the moment is the same for revolution as for pure translation. The forces result from combined translation and rotation; the moment from translation oblique to the axes a, b , irrespective of rotational speed.

COMBINATION OF APPLIED FORCES.—To find the whole applied force constraining a body to uniform circular motion in a perfect fluid (55), (60) may be added, or graphs like those of Figures 11, 12, may be superposed. For an airship having $m_1 = m$, (55), (60) give

$$\bar{X} = -(1 + k_b) m v r \quad \bar{Y} = (1 + k_a) m u r \quad \bar{N} = (k_b - k_a) m u v \quad (64)$$

* Writing $R = r Q \cdot m \sqrt{k_a^2 \cos^2 \alpha + k_b^2 \sin^2 \alpha}$ we may call it the centripetal force of the apparent mass $m \sqrt{k_a^2 \cos^2 \alpha + k_b^2 \sin^2 \alpha}$ for the body direction of Q .

$$X = -\pi a^2 \rho r v \quad Y = \pi b^2 \rho r u \quad N = \pi(a^2 - b^2) \rho \cdot uv = \pi(a^2 - b^2) \frac{\rho Q^2}{2} \sin 2\alpha \quad (65)$$

The resultant force $\pi \rho r \sqrt{a^2 v^2 + b^2 u^2}$ has the slope $-b^2 u/a^2 v = -b^2/a^2 \cot \alpha$; the central axis is through the path center; X is the same as for a round cylinder of radius a ; Y the same as for one of radius b . For a good elliptic aircraft strut $a/b=3$; hence $X/Y = -9v/u = -9 \tan \alpha$; $N = 8\pi b^2 \rho uv = 8\pi b^2 \cdot \frac{\rho Q^2}{2} \cdot \sin 2\alpha$. By (65) N is the same for all confocal elliptic cylinders, since $a^2 - b^2$ is so.

If $a=b$, as for a round strut, $N=0$, $R = \pi a^2 \rho r Q^2$ and coincides with the body's previously found centripetal force to which it bears the ratio m/m_1 .

If $b=0$, as for a flat plate, (65) become

$$X = -\pi a^2 \rho r v \quad Y = 0 \quad N = \pi a^2 \rho uv = \pi a^2 \frac{\rho Q^2}{2} \sin 2\alpha \quad (66)^*$$

The equivalent resultant force $\pi a^2 \rho r v$, with slope $Y/X = -0$, runs through the path center parallel to x . If $r=0$, the plate has pure translation, with forces $X, Y=0$, and moment $N = \pi a^2 \rho uv$, a well known result. X in (66), being the same as in (65), is independent of the strut thickness b .

(2) For a prolate spheroid, of semiaxes a, b, b , in uniform yawing flight, $m = 4/3 \cdot \pi \rho a b^2$, and k_a, k_b are as given in Table III. Thus for $a/b=4$, $k_a, k_b = 0.082, 0.860$; hence by (60)

$$X = -3.6ab^2 \rho r v \quad Y = 0.3434ab^2 \rho r u \quad N = 3.26ab^2 \rho uv \quad (67)$$

(3) For an elliptic disk of semiaxes a, b, c , moving as in Figure 14, Table VIII gives $k_c m = \frac{4}{3} \pi \rho a b^2 / E$; hence by (57) the forces and moment are

$$Y = -k_c m p w = -\frac{4a}{3E} \pi \rho b^2 \cdot p w \quad Z = 0$$

$$L = k_c m \cdot v w = \frac{4a}{3E} \pi \rho b^2 \cdot v w \quad (68)$$

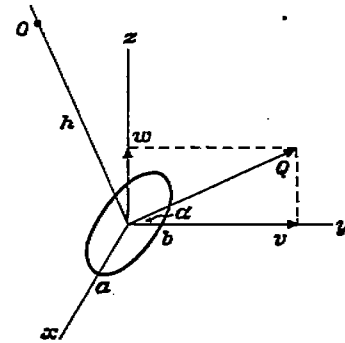


FIGURE 14.—Thin elliptic wing moving parallel to its plane of symmetry through a perfect fluid

the other pertinent terms in (57) vanishing, as appears on numerical substitution. Here $E = E\left(\theta, \frac{\pi}{2}\right)$, $\sin^2 \theta = (a^2 - b^2)/a^2$; also $L = \frac{4a}{3E} \pi \rho b^2 \frac{\rho Q^2}{2} \sin 2\alpha$. Compare (68) with (66), calling b the width in both.

THEORY VERSUS EXPERIMENT.—In favorable cases the moment formulas of Part IV accord fairly well with experiment, as the following instances show. For lack of available data the force formulas for curvilinear motion are not compared with experiment.

(1) By (65) an endless elliptic strut with $a=1/3$ foot, $b=1/12$ foot, $c=5$ feet, held at α degrees incidence in a uniform stream of standard air at 40 miles an hour, for which $\rho Q^2/2 = 4.093$ pounds per square foot, sustains the yawing moment per foot length

$$N = \pi(a^2 - b^2) \cdot \frac{\rho Q^2}{2} \cdot \sin 2\alpha = 1.3392 \sin 2\alpha \text{ lb. ft.} \quad (69)$$

This compares with the values found in the Navy 8 by 8 foot tunnel, as shown in Table IX faired from Figure 15. The agreement is approximate for small angles of attack. The model was of varnished mahogany, and during test was held with its long axis c level across stream, and with two closely adjacent sheet metal end plates, 2 feet square, to give the effect of plane flow.

* Equations (66) were published in Reference 5 as the result of a special research to determine the fluid forces and moment on a revolving plate. In the present text they follow as corollaries from more general formulas.

(2) By (66) an endless thin flat plate of width $2a=5/12$ feet, similarly held in the same air stream, has per unit length the moment

$$N = \pi a^2 \frac{\rho Q^2}{2} \sin 2\alpha = 0.5581 \sin 2\alpha \text{ lb. ft.} \quad (70)$$

This is compared in Table X and Figure 16 with the values found in the Navy 8 by 8 foot tunnel. The flat plate was of polished sheet aluminum $3/32$ inch thick, with half round edges front and rear.

Again for an endless flat steel plate 5.95 inches wide by 0.178 inch thick at the center, with its front face flat and back face V-tapered to sharp edges, Fage and Johansen, Reference 6,

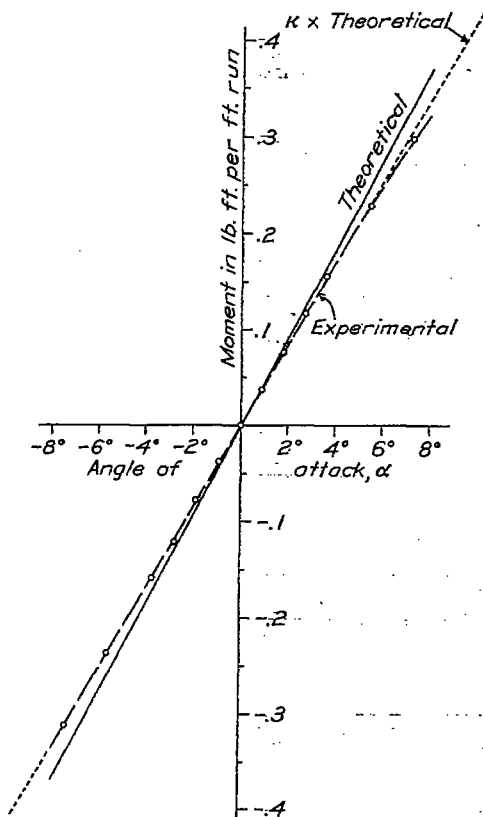


FIGURE 15.—Theoretical and experimental moment about long axis of endless elliptic cylinder. Width 8 inches, thickness 2 inches, air speed 40 miles per hour. Correction factor $\kappa=0.912$

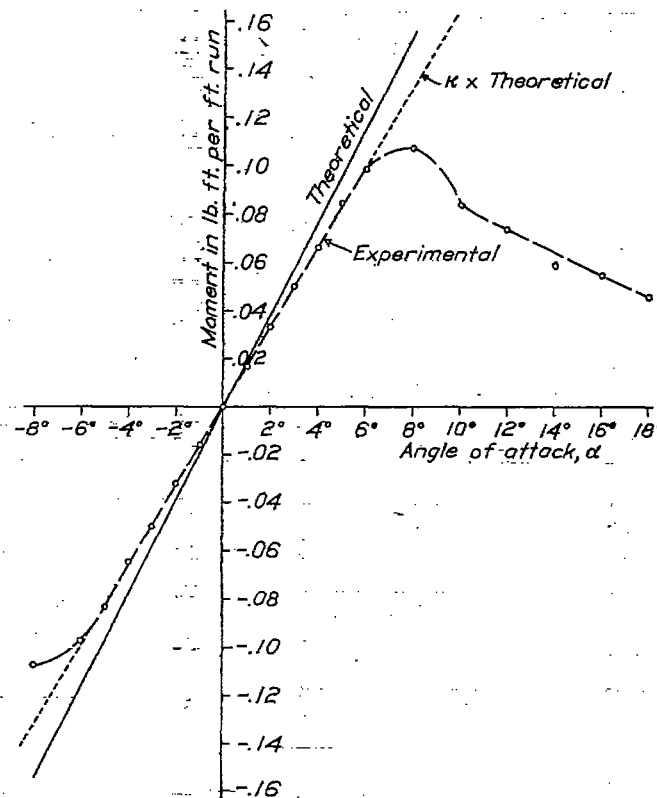


FIGURE 16.—Theoretical and experimental moment about long axis of endless rectangular plate. Width 5 inches, air speed 40 miles per hour. Correction factor $\kappa=0.800$

found, at 50 feet per second and 5.85° angle of attack, $N=0.125$ pound foot as the moment per foot run about the long axis, computed from the measured pressure over the median section. By (66), a thin flat plate would have

$$N = \pi a^2 \cdot \frac{\rho Q^2}{2} \cdot \sin 2\alpha = 0.1931 \times 2.9725 \times 0.2028 = 0.116 \text{ lb. ft.}$$

which is 7 per cent less than 0.125 found with their slightly cambered plate.

(3) An elliptic disk $3/32$ inch thick with $a, b=15, 2.5$ inches, when held as a wing in the Navy 40-mile-an-hour stream, had the moment L versus angle of attack α shown in Figure 17 and Table XI. For this case

$$\sin^2 \theta = (a^2 - b^2)/a^2 = 875/900, \quad \theta = 80^\circ - 24', \quad E = 1.03758.$$

Also in (68) $a=5/4$ feet, $b=5/24$ feet, $Q^2=4.093$; hence

$$L = \frac{4a}{3E} \cdot \pi b^2 \cdot \frac{\rho Q^2}{2} \cdot \sin 2\alpha = 0.8963 \sin 2\alpha \text{ lb. ft.} \quad (71)$$

which gives the theoretical values in Figure 17 and Table XI. The agreement is fair at small incidences. The disk as tested was of sheet aluminum cut square at the edges without any rounding or sharpening.

(4) For a wooden prolatespheroid 24 inches long by 6 inches thick, carried as in Figure 12 round a circle of radius $h=27.96$ feet to the model's center, Jones, Reference 3, found at 40 feet per second the values of N listed in Table XII. For this case Table III gives $k_b - k_a = 0.778$, and (61) gives

$$N = (k_b - k_a) \tau \cdot \frac{\rho Q^2}{2} \cdot \sin 2\alpha = 0.388 \sin 2\alpha.$$

These values appear from Table XII not to accord closely with the experimental ones.

CORRECTION FACTORS.—Figures 15, 16, 17 portray experimental moments, at small angles, as accurately equal to the theoretical times an empirical correction factor κ . Thus amended (61) gives for the experimental moment

$$N_e = \kappa N = \kappa (k_b - k_a) \tau \cdot \frac{\rho Q^2}{2} \cdot \sin 2\alpha.$$

For the given elliptical cylinder $\kappa = 0.912$ with $-8^\circ < \alpha < 6^\circ$; for the endless plate $\kappa = 0.860$ with $-6^\circ < \alpha < 6^\circ$; for the elliptic disk $\kappa = 0.887$ with $-5^\circ < \alpha < 4^\circ$. In such cases one should expect to find the actual air pressure nearly equal to the theoretical over the model's forward part, but so deficient along the rear upper surface as to cause a

defect of resultant moment. No effort is made here to estimate it theoretically, nor to determine it empirically for a wide range of conditions.

The measurements shown in Table X, for the flat plate, were repeated at 50 and 60 miles an hour without perceptible scale effect.

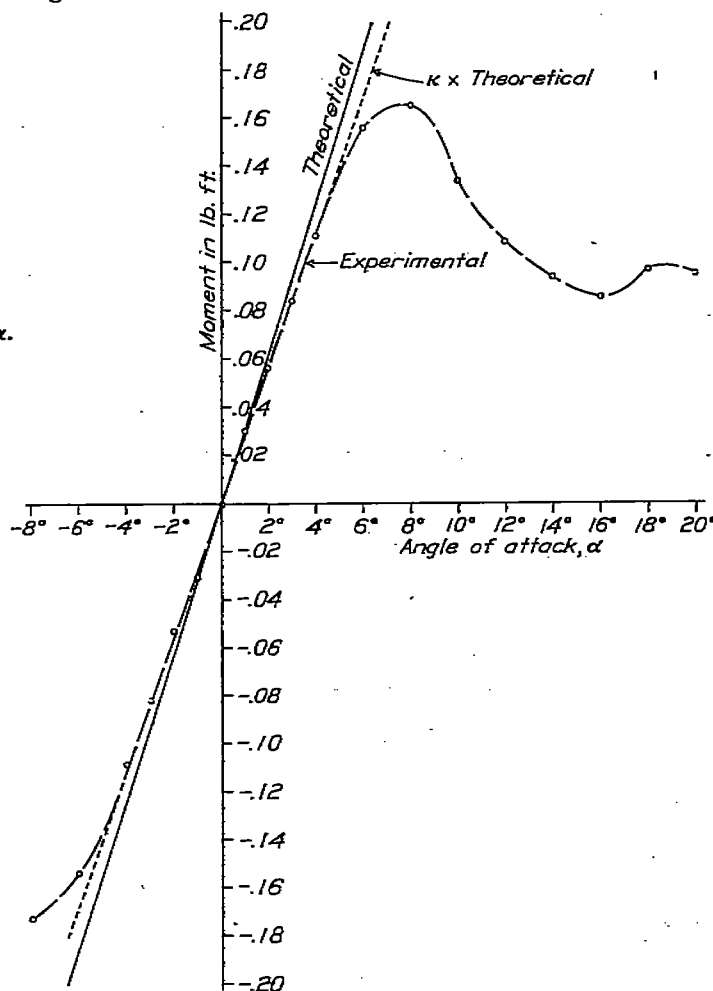


FIGURE 17.—Theoretical and experimental moment about long axis of elliptic disk. Length 30 inches, width 5 inches, air speed 40 miles per hour. Correction factor $\kappa = 0.887$

REPORT No. 323

FLOW AND FORCE EQUATIONS FOR A BODY REVOLVING IN A FLUID

PART V

POTENTIAL COEFFICIENTS, INERTIA COEFFICIENTS

GREEN'S INTEGRALS.—The foregoing text employs Green's well-known integrals, which for the ellipsoid abc may be symbolized thus:

$$\alpha = abc \int_{\lambda}^{\infty} \frac{d\lambda}{a'^3 b' c'}, \quad \beta = abc \int_{\lambda}^{\infty} \frac{d\lambda}{a' b'^3 c'}, \quad \gamma = abc \int_{\lambda}^{\infty} \frac{d\lambda}{a' b' c'^3} \quad (72)$$

where $a' = \sqrt{a^2 + \lambda}$, $b' = \sqrt{b^2 + \lambda}$, etc., are semiaxes of the confocal ellipsoid $a'b'c'$. The integrals have the following values, Reference 4:

$$\left. \begin{aligned} \alpha &= A(b^2 - c^2)[F(\theta, \varphi) - E(\theta, \varphi)] \\ \beta &= A(c^2 - a^2) \left[\frac{b^2 - c^2}{a^2 - c^2} F(\theta, \varphi) + \frac{a^2 - b^2}{\sqrt{a^2 - c^2}} \frac{c'}{a' b'} - E(\theta, \varphi) \right] \\ \gamma &= A(a^2 - b^2) \left[\sqrt{a^2 - c^2} \frac{b'}{a' c'} - E(\theta, \varphi) \right] \end{aligned} \right\} \quad (73)^1$$

where

$$A = \frac{2abc}{(a^2 - b^2)(b^2 - c^2)\sqrt{a^2 - c^2}}, \quad \sin^2 \theta = \frac{a^2 - b^2}{a^2 - c^2}, \quad \sin^2 \varphi = \frac{a^2 - c^2}{a^2 + \lambda} \quad (74)$$

and the elliptic integrals are

$$F(\theta, \varphi) = \int (1 - \sin^2 \theta \sin^2 \varphi)^{-1/2} d\varphi, \quad E(\theta, \varphi) = \int (1 - \sin^2 \theta \sin^2 \varphi)^{1/2} d\varphi \quad (75)$$

Numerical values of $F(\theta, \varphi)$, $E(\theta, \varphi)$, α , β , γ are given in Tables I, II for $\lambda=0$ and various ratios a/b , b/c ; viz, for various shapes of the ellipsoid abc . For $\varphi = \pi/2$ one writes $F(\theta, \varphi) = K$, $E(\theta, \varphi) = E$, by convention.

POTENTIAL COEFFICIENTS.—For motion (49) the ellipsoid abc has the potential coefficients known from textbooks.

$$\left. \begin{aligned} m_a &= \frac{\alpha}{2 - \alpha_0} & m'_a &= \frac{G(\gamma - \beta)}{2G - (\gamma_0 - \beta_0)} \text{ where } G = \frac{b^2 - c^2}{b^2 + c^2} \\ m_b &= \frac{\beta}{2 - \beta_0} & m'_b &= \frac{H(\alpha - \gamma)}{2H - (\alpha_0 - \gamma_0)} \text{ where } H = \frac{c^2 - a^2}{c^2 + a^2} \\ m_c &= \frac{\gamma}{2 - \gamma_0} & m'_c &= \frac{I(\beta - \alpha)}{2I - (\beta_0 - \alpha_0)} \text{ where } I = \frac{a^2 - b^2}{a^2 + b^2} \end{aligned} \right\} \quad (76)$$

m_a , m_b , m_c being for translation along a , b , c and m'_a , m'_b , m'_c for rotation about them, and α_0 , β_0 , γ_0 being (73) for $\lambda=0$; viz, for a' , b' , $c'=a$, b , c . Surface values of (76), viz, for α , β , $\gamma = \alpha_0$, β_0 , γ_0 are given in Tables III, IV. For fluid inside the ellipsoid the potential coefficients are as in (40) and given numerically in Table V.

INERTIA COEFFICIENTS.—From (76) are derived the conventional linear and angular inertia coefficients

$$k_a, k_b, k_c = m_a, m_b, m_c \quad k'_a, k'_b, k'_c = Gm'_a, Hm'_b, Im'_c \quad (77)$$

for the ellipsoid moving through or containing liquid, as in (40), (49). Surface values are given in Tables III, VI, VII.

¹ (73) satisfy the known relation $\alpha + \beta + \gamma = 2abc/a'b'c'$, as appears on adding.

LIMITING CONDITIONS.—In some limiting cases, as for $c=0$, or $a=b$, etc., (73) may become indeterminate and require evaluation, as in Reference 4. In such cases the formulas in Table VIII may be used. For $c=0$, entailing zero mass and infinite k_c , k'_a , k'_b , one may use in (57) the values of $k_c m$, $k'_a A$, $k'_b B$ given at the bottom of Table VIII.

PHYSICAL MEANING OF THE COEFFICIENTS.—The tabulated potential coefficients, put in (40) or (49), serve to find the numerical value of the potential φ , or impulse $-\rho\varphi$ per unit area, at any point (x, y, z) of an ellipsoid surface.² Integration of $\rho\varphi$ over any surface, as explained for p in Part I, gives the component linear and angular zonal impulses. So, too, integration of $-\rho\varphi q_n/2$, where q_n is the normal surface velocity at (x, y, z) , gives the kinetic energy imparted to the fluid; and integration of the impulsive pressure $-\rho\partial\varphi/\partial t$ gives the impulsive zonal forces and moments. One finds $\rho\partial\varphi/\partial t$ for (40), (49) by using with them the specified density ρ , accelerations \dot{U} , \dot{V} , \dot{W} , $\dot{\Omega}_a$, $\dot{\Omega}_b$, $\dot{\Omega}_c$, and tabulated potential coefficients for the given semiaxes a , b , c .

Thus putting $-\rho\varphi_c$, $-\rho\varphi'_c$ for p in (9), (10₁), and integrating over the whole ellipsoid surface, easily gives the fluid's linear and angular momenta

$$k_c m W \quad k'_c C \Omega_c \text{-----} (78)$$

where $m W$, $C \Omega_c$ are respectively the linear and angular momenta of the displaced fluid moving as a solid with velocities W , Ω_c . The like surface integration of $-\rho\varphi_c q_n/2$ gives, as is well known,

$$k_c m W^2/2 \quad k'_c C \Omega_c^2/2 \text{-----} (79)$$

where $m W^2/2$, $C \Omega_c^2/2$ are the kinetic energies of the displaced fluid so moving. Each inertia coefficient therefore is a ratio of the body's apparent inertia, due to the field fluid, to the like inertia of the displaced fluid moving as a solid.

By (49) the potential coefficients due to velocities W , Ω_c are

$$m_c = -\varphi_c/Wz \quad m'_c = -\varphi'_c/\Omega_c xy$$

The first is the ratio of the outer and inner surface potentials due to W at any point z on the ellipsoid abc ; the second is the ratio of the potentials due to Ω_c at (x, y) , respectively on the outer surface of that ellipsoid and inside the cylinder of semiaxes a , b , c .

One notes that the momenta (78) times half the velocities give (79); also that the time derivatives of (78) are the force and moment Z , $N = k_c m \dot{W}$, $k'_c C \dot{\Omega}_c$, as in (57) for the simple z -wise motions, \dot{W} , $\dot{\Omega}$.

For any axial surface, say of torpedo form, moving as in Figure 12, the ratio $-k'_c C \Omega_c/k_c m V$ is the distance from the arbitrary origin O_1 to the impulse center O_2 , or center of virtual mass. This may be taken as origin, and if the body's center of mass also is there Figures 11, 12 can still be superposed as in Figure 13. In the same way are related the acceleration force and moment $k_c m \dot{V}$, $k'_c C \dot{\Omega}_c$, thus illustrating the doctrine that the motion of a hydrokinetically symmetric form in a boundless perfect fluid, without circulation, obeys the ordinary dynamic equations for a rigid body.

AERODYNAMICAL LABORATORY,

BUREAU OF CONSTRUCTION AND REPAIR, U. S. NAVY;

WASHINGTON, D. C., December 17, 1928.

² This impulse is imparted by the moving surface to the fluid, otherwise still; the fluid in turn tends to impart to the body the impulse $\rho\varphi$ per unit area at (x, y, z) .

CHIEF SYMBOLS USED IN THE TEXT

GEOMETRICAL

a, b, c -----	Semiaxes of ellipsoid abc .
a', b', c' -----	Semiaxes of confocal ellipsoid $a'b'c'$.
e, e' -----	Eccentricities of ellipse ab and its confocal $a'b'$; $ae = a'e' = \sqrt{a^2 - b^2}$.
$n; h_1, h_2$ -----	Normal to ellipse ab ; distances from origin to normal and tangent.
l, m, n -----	Direction cosines of normal n to any surface.
$s; s_\eta, s_\alpha$ -----	Length along any line; lengths along meridian and circle of latitude.
x, y, z -----	Cartesian coordinates; also coordinate axes.
r, β, ω -----	Polar coordinates of prolate spheroid abc .
η, θ -----	Eccentric angle of ab , inclination to x of normal to ab .

KINEMATICAL

u, v, w -----	Component velocities of fluid parallel to x, y, z axes.
q_n, q_a -----	Component velocities of fluid parallel to tangent and normal.
q_o, q -----	Resultant velocity of fluid before and after disturbance.
u, v, w -----	Component translation velocities of abc parallel to a, b, c
U, V, W -----	Component translation velocities of abc parallel to a, b, c
p, q, r -----	Component rotation velocities of abc about a, b, c -----
$\Omega_a, \Omega_b, \Omega_c$ -----	Component rotation velocities of abc about a, b, c -----
φ, ψ -----	Velocity potential, stream function.
m_a, m_b, m_c -----	Potential coefficients for abc with velocities u, v, w or U, V, W .
m'_a, m'_b, m'_c -----	Potential coefficients for abc with velocities p, q, r or $\Omega_a, \Omega_b, \Omega_c$.
$Q = \sqrt{U^2 + V^2 + W^2}$ -----	Resultant velocity of abc .

Alternative symbols.

DYNAMICAL

A_1, B_1, C_1 -----	Moments of inertia of rigid body about its axes a, b, c .
A, B, C -----	Moments of inertia of displaced fluid moving as a solid.
m_1, m -----	Mass of body, mass of displaced fluid.
ρ, τ -----	Density of fluid, volume of model or displaced fluid.
p, p_a -----	Pressure of fluid moving, pressure on coming to rest.
$X_1, Y_1, Z_1; R_1$ -----	Component forces applied to free rigid body; resultant force.
$X, Y, Z; R$ -----	Component forces exerted by body on fluid; resultant force.
L_1, M_1, N_1 -----	Component moments about a, b, c applied to rigid body.
L, M, N -----	Component moments about a, b, c exerted by body on fluid.
k_a, k_b, k_c -----	Inertia coefficients for abc moving parallel to a, b, c in fluid.
k'_a, k'_b, k'_c -----	Inertia coefficients for abc rotating about a, b, c in fluid.

REFERENCES

- Reference 1. Lamb, H.: Hydrodynamics, 5th ed., 1924. On the Forces Experienced by a Solid Moving Through a Liquid. Quart. Journ. Math. t. XIX (1883).
- Reference 2. Zahm, A. E.: Flow and Drag Formulas for Simple Quadrics. Report No. 253, National Advisory Committee for Aeronautics, 1927.
- Reference 3. Jones, R.: The Distribution of Normal Pressures on a Prolate Spheroid. R. & M. No. 1061, British Aeronautical Research Committee, 1925.
- Reference 4. Tuckerman, L. B.: Inertia Factors of Ellipsoids for Use in Airship Design. Report No. 210, National Advisory Committee for Aeronautics, 1925.
- Reference 5. Cardonazzo, B.: Über die gleichförmige Rotation eines festen Körpers in einer unbegrenzten Flüssigkeit. In Vorträge, etc., edited by Karman & Levi-Civita, 1924.
- Reference 6. Fage and Johansen: On the Flow of Air Behind an Inclined Flat Plate of Infinite Span. R. & M. No. 1104, British Aeronautical Research Committee, 1927.
- Reference 7. Larmor, J.: On Hydrokinetic Symmetry. Quart. Journ. Math. t. XX (1920).
- Reference 8. Ames, J. S.: A Résumé of the Advance in Theoretical Aeronautics made by Max M. Munk. Report No. 213, National Advisory Committee for Aeronautics, 1925.

TABLE I
ELLIPTIC INTEGRALS $F(\theta, \varphi)$, $E(\theta, \varphi)$ ¹
[Defined in eq. (75), Part VI]

a/c	b/c										
	1	2	3	4	5	6	7	8	9	10	∞
$F(\theta, \varphi)$											
1	0.00000										
2	1.81828	1.04720									
3	1.78305	1.43870	1.23095								
4	2.08412	1.71374	1.48399	1.31814							
5	2.29319	1.92798	1.68471	1.50687	1.36940						
6	2.47903	2.10413	1.85188	1.66560	1.62053	1.40832					
7	2.63508	2.25400	1.98520	1.80281	1.63204	1.62940	1.42745				
8	2.77024	2.38432	2.12075	1.92379	1.78356	1.64194	1.53595	1.44550			
9	2.89035	2.49971	2.23265	2.03191	1.87318	1.74321	1.63405	1.54065	1.45948		
10	2.99838	2.60258	2.33303	2.12855	1.96504	1.83534	1.72357	1.62768	1.54419	1.47063	
∞	∞	∞	∞	∞	∞	∞	∞	∞	∞	∞	∞
$E(\theta, \varphi)$											
1	0.00000										
2	.88803	1.04720									
3	.84277	1.07024	1.23095								
4	.80522	1.09091	1.18103	1.31814							
5	.77575	1.05019	1.14337	1.25126	1.36940						
6	.75397	1.04146	1.11604	1.20294	1.29896	1.40832					
7	.73872	1.03472	1.09559	1.16833	1.24893	1.33574	1.42745				
8	.72714	1.02946	1.08071	1.14185	1.21035	1.28451	1.36317	1.44550			
9	.71878	1.02529	1.06594	1.12136	1.18040	1.24464	1.31304	1.38453	1.45948		
10	.71296	1.02195	1.05996	1.10516	1.15869	1.21297	1.27310	1.33642	1.40240	1.47063	
∞	1.00000	1.00000	1.00000	1.00000	1.00000	1.00000	1.00000	1.00000	1.00000	1.00000	1.00000

¹ The integrals in this table are culled from L. Potin's Formules et Tables Numerique.

TABLE II
GREEN'S INTEGRALS $\alpha_0, \beta_0, \gamma_0$
[Defined in eq. (73), Part VI]

a/c	b/c										
	1	2	3	4	5	6	7	8	9	10	∞
α_0											
1	0.66667										
2	.34713	0.47280									
3	.21761	.31265	0.36460								
4	.15082	.22474	.26820	0.29636							
5	.11171	.17064	.20719	.23189	0.24951						
6	.086327	.13471	.16584	.18769	.20536	0.21541					
7	.069266	.10950	.13629	.15541	.16970	.18950	0.19914				
8	.056894	.091037	.11435	.13125	.14426	.16440	.18254	0.19914			
9	.047710	.077071	.097571	.11276	.12448	.13378	.14132	.14757	0.15271		
10	.043637	.066203	.084381	.097957	.10872	.11728	.12428	.13010	.13500	0.13920	
∞	0	0	0	0	0	0	0	0	0	0	0
β_0											
1	0.66667										
2	.32643	0.47280									
3	.39127	.53423	0.36460								
4	.32459	.50564	.39662	0.29636							
5	.24418	.50182	.41804	.31587	0.24951						
6	.19578	.40693	.43307	.32965	.26265	0.21541					
7	.16538	.31775	.44413	.34083	.27275	.22477	0.18950				
8	.14184	.23277	.45260	.34912	.28071	.23234	.19654	0.16914			
9	.127619	.23184	.45913	.35569	.28709	.23847	.20237	.17458	0.15271		
10	.117972	.23859	.46437	.36109	.29233	.24364	.20725	.17927	.15712	0.13920	
∞	1.00000	.66667	.50000	.40000	.33333	.28572	.25000	.22222	.20000	.18182	0
γ_0											
1	0.66667										
2	.82643	1.05440									
3	.89127	1.18312	1.27078								
4	.92459	1.26572	1.33518	1.40726							
5	.94418	1.29752	1.37478	1.45223	1.50068						
6	.95378	1.29835	1.40110	1.48287	1.53401	1.56918					
7	.96338	1.27273	1.41956	1.50377	1.55754	1.60443	1.62100				
8	.97154	1.25320	1.43506	1.51953	1.57504	1.61325	1.64091	1.66173			
9	.97619	1.26109	1.44329	1.53154	1.58344	1.62775	1.65630	1.67784	1.69457		
10	.97972	1.26720	1.45125	1.54094	1.59395	1.63917	1.66846	1.69062	1.70787	1.72160	
∞	1.00000	1.33333	1.50000	1.60000	1.66667	1.71429	1.75000	1.77778	1.80000	1.81818	2.00000

TABLE III
POTENTIAL COEFFICIENTS m_a , m_b , m_c * FOR ELLIPSOIDS IN TRANSLATION

(For outer surface of $a b c$)

[Defined in eq. (76)]

a/c	b/c										
	1	2	3	4	5	6	7	8	9	10	∞
m_a											
1	0.5000										
2	.2100	0.3096									
3	.1220	.1853									
4	.08162	.1266	0.2229								
5	.05916	.09328	.1549	0.1740							
6	.04532	.07222	.1166	.1312	0.1425						
7	.03588	.05722	.09042	.1036	.1132	0.1207					
8	.02828	.04769	.07313	.08425	.09272	.09838	0.1047				
9	.02444	.04008	.06064	.07029	.07774	.08366	.08846	0.09238			
10	.02074	.03423	.05129	.05975	.06637	.07169	.07608	.07966	0.08267		
∞	0	0	0	0	0	0	0	0	0	0.07481	0
m_b											
1	0.5000										
2	.7042	0.3096									
3	.8039	.3945	0.2229								
4	.8598	.3963	.2474	0.1740							
5	.8943	.4203	.2643	.1876	0.1425						
6	.9171	.4367	.2764	.1974	.1512	0.1207					
7	.9331	.4489	.2855	.2054	.1579	.1266	0.1047				
8	.9447	.4554	.2925	.2115	.1633	.1314	.1090	0.09238			
9	.9535	.4618	.2980	.2162	.1676	.1354	.1128	.09564	0.08267		
10	.9603	.4676	.3024	.2203	.1712	.1387	.1156	.09846	.08526	0.07481	
∞	1.0000	.5000	.3333	.2500	.2000	.1667	.1429	.12500	.11111	.10000	0
m_c											
1	0.5000										
2	.7042	1.115									
3	.8039	1.362	1.743								
4	.8598	1.618	2.008	2.374							
5	.8943	1.823	2.199	2.651	3.008						
6	.9171	1.997	2.339	2.866	3.282	3.642					
7	.9331	1.750	2.440	3.030	3.530	3.951	4.277				
8	.9447	1.790	2.528	3.183	3.706	4.171	4.570	4.912			
9	.9535	1.821	2.593	3.269	3.860	4.378	4.819	5.203	5.548		
10	.9603	1.846	2.645	3.357	3.967	4.543	5.032	5.465	5.846	6.184	
∞	1.0000	2.000	3.000	4.000	5.000	6.000	7.000	8.000	9.000	10.000	∞

* These have the same values as the inertia coefficients k_a , k_b , k_c .

TABLE IV
POTENTIAL COEFFICIENTS m'_a , m'_b , m'_c FOR ELLIPSOIDS IN ROTATION
(For outer surface of $a b c$)

[Defined in eq. (76)]

a/c	b/c										
	1	2	3	4	5	6	7	8	9	10	∞
	m'_a										
1	0										
2	0	0.5643									
3	0	.6390	1.045								
4	0	.6768	1.135	1.499							
5	0	.6989	1.190	1.536	1.943						
6	0	.7125	1.225	1.663	2.042	2.390					
7	0	.7211	1.249	1.705	2.113	2.481	2.813				
8	0	.7270	1.266	1.738	2.165	2.556	2.915	3.245			
9	0	.7315	1.278	1.762	2.205	2.616	2.995	3.343	3.675		
10	0	.7348	1.288	1.780	2.235	2.660	3.038	3.430	3.778	4.108	
∞	0	.7500	1.333	1.875	2.400	2.917	3.429	3.937	4.444	4.950	∞
	m'_b										
1	0										
2	-0.3990	-0.5643									
3	-.6819	-.8833	-1.045								
4	-.6898	-1.104	-1.349	-1.499							
5	-.7581	-1.264	-1.688	-1.900	-1.943						
6	-.8058	-1.384	-1.780	-2.052	-2.243	-2.390					
7	-.8402	-1.476	-1.935	-2.264	-2.504	-2.680	-2.813				
8	-.8659	-1.543	-2.062	-2.445	-2.732	-2.948	-3.114	-3.245			
9	-.8857	-1.607	-2.168	-2.600	-2.931	-3.188	-3.488	-3.647	-3.675		
10	-.9013	-1.654	-2.257	-2.734	-3.107	-3.402	-3.637	-3.825	-3.978	-4.108	
∞	-1.0000	-2.000	-3.000	-4.000	-5.000	-6.000	-7.000	-8.000	-9.000	-10.000	$-\infty$
	m'_c										
1	0										
2	0.3990	0									
3	.6819	0.1556	0								
4	.6898	.2420	0.08332	0							
5	.7581	.2969	.1359	0.05193	0						
6	.8058	.3350	.1719	.08705	0.03549	0					
7	.8402	.3627	.1981	.1134	.06127	0.02509	0				
8	.8659	.3836	.2181	.1330	.08081	.04529	0.01951	0			
9	.8857	.3993	.2335	.1494	.09610	.06025	.03436	0.01327	0		
10	.9013	.4127	.2460	.1608	.1084	.07291	.04721	.02770	0.01238	0	
∞	1.0000	.6000	.3333	.2500	.2000	.16667	.14286	.12500	.11111	0.10000	0

TABLE VI
INERTIA COEFFICIENTS¹ k'_a, k'_b, k'_c FOR ELLIPSOIDS IN ROTATION

(For outer surface of $a b c$)

[Defined in eq. (77)]

a/c	b/c										
	1	2	3	4	5	6	7	8	9	10	∞
$k'_a = Gm'_a$											
1	0										
2	0	0.3356									
3	0	.3834	0.8359								
4	0	.4081	.9081	1.323							
5	0	.4194	.9519	1.408	1.793						
6	0	.4275	.9893	1.468	1.885	2.251					
7	0	.4326	.9995	1.505	1.950	2.347	2.701				
8	0	.4362	1.013	1.533	1.999	2.418	2.799	3.145			
9	0	.4389	1.023	1.555	2.035	2.473	2.875	3.245	3.585		
10	0	.4409	1.030	1.571	2.064	2.515	2.935	3.324	3.686	4.022	
∞	0	.4500	1.067	1.654	2.215	2.759	3.291	3.816	4.336	4.852	∞
$k'_b = Hm'_b$											
1	0										
2	0.2394	0.3356									
3	.4655	.7082	0.8359								
4	.6078	.9745	1.191	1.323							
5	.6998	1.167	1.466	1.662	1.793						
6	.7622	1.309	1.653	1.941	2.122	2.251					
7	.8066	1.417	1.857	2.174	2.403	2.573	2.701				
8	.8393	1.501	1.999	2.370	2.648	2.857	3.019	3.145			
9	.8641	1.567	2.115	2.536	2.860	3.110	3.305	3.460	3.585		
10	.8834	1.622	2.213	2.679	3.045	3.335	3.565	3.749	3.900	4.022	
∞	1.0000	2.000	3.000	4.000	5.000	6.000	7.000	8.000	9.000	10.000	∞
$k'_c = Im'_c$											
1	0										
2	0.2394	0									
3	.4655	0.05985	0								
4	.6078	.1452	0.02333	0							
5	.6998	.2150	.06383	0.01140	0						
6	.7622	.2690	.1031	.03345	0.00540	0					
7	.8066	.3079	.1367	.05758	.01987	0.00393	0				
8	.8393	.3385	.1643	.07982	.03641	.01268	0.00259	0			
9	.8641	.3622	.1869	.09941	.05077	.02330	.00858	0.00179	0		
10	.8834	.3810	.2054	.1164	.06503	.03431	.01616	.00608	0.00120	0	
∞	1.0000	.5000	.3333	.2500	.20000	.16667	.14286	.12500	.11111	0.10000	0

¹ For translation k_a, k_b, k_c are given in Table III.

TABLE VII—
INERTIA COEFFICIENTS k'_a , k'_b , k'_c FOR ELLIPSOIDS IN ROTATION.

(Inner surface of $a b c$)

[Defined in eq. (77)]

[illegible]

TABLE VIII
INERTIA VALUES FOR LIMITING FORMS OF ELLIPSOIDS $a > b > c$

INERTIA COEFFICIENTS FOR TRANSLATION AND ROTATION							
a/b	Shape	k_x	k_b	k_z	k'_x	k'_b	k'_z
$c=0$							
1	Circular disk	0	0	∞	∞	∞	0
1+	Elliptical disk	0	0	∞	∞	∞	0
∞	Long rectangle	0	0	∞	∞	∞	0
$b > c > 0$							
1	Oblate spheroid $e^2 = 1 - c^2/a^2$	$\frac{c}{a} \frac{ce - a \sin^{-1}e}{ae(e^2+1) - c \sin^{-1}e}$	$\frac{a}{c} \frac{ae - c \sin^{-1}e}{ce - a \sin^{-1}e}$	$\frac{e^2(\gamma_0 - \beta_0)}{(2-e^2)[2e^2 - (2-e^2)(\gamma_0 - \beta_0)]}$			0
1+	Ellipsoid						
∞	Elliptical cylinder	0	c/b	b/c	$\frac{1}{2} \frac{(b^2 - c^2)}{b^2 + c^2}$	b/c	c/b
$c=b$							
1	Sphere	$\frac{1}{2}$	$\frac{1}{2}$	$\frac{1}{2}$	0	0	0
1+	Prolate spheroid $e^2 = 1 - c^2/a^2$	$\frac{\log_e \frac{1+e}{1-e} - 2e}{\log_e \frac{1+e}{1-e} - 2e}$	$\frac{\log_e \frac{1+e}{1-e} - 2e}{\log_e \frac{1+e}{1-e} - 2e}$	$\frac{\log_e \frac{1+e}{1-e} - 2e}{\log_e \frac{1+e}{1-e} - 2e}$	0	$\frac{e^2(\beta_0 - \alpha_0)}{(2-e^2)[2e^2 - (2-e^2)(\beta_0 - \alpha_0)]}$	
∞	Round cylinder	0	1	1	0	1	1
APPARENT MASSES AND MOMENTS OF INERTIA WHEN $c=0$							
a/b	Shape	k_{xm}	k_{bm}	k_{zm}	k'_{xI}	k'_{bB}	k'_{zC}
1	Circular disk	0	0	$\frac{8}{3} \rho a^2$	$\frac{16}{45} \rho a^2$		0
1+	Elliptical disk	0	0	$\frac{4}{3} \pi \rho ab^2/E$	$\frac{4\pi\rho}{15} \frac{ab^2(a^2-b^2)}{(a^2-b^2)E - b^2K}$	$\frac{4\pi\rho}{15} \frac{a^2b^2(a^2-b^2)}{(a^2-2b^2)E + b^2K}$	0
∞	Long rectangle $a=\infty$	0	0	$\pi \rho b^2$	$\frac{1}{3} \pi \rho b^2$	$\frac{1}{3} \pi \rho b^2$	0

$$\gamma_0 - \beta_0 = -1 + \frac{3}{e^2} \frac{3}{2} \sqrt{1-e^2} \sin^{-1}e$$

$$\beta_0 - \alpha_0 = -2 + \frac{3}{e^2} \frac{3}{2} \frac{1-e^2}{e^2} \log_e \frac{1+e}{1-e}$$

* Per unit length of model.

TABLE IX
LIFT, DRAG, AND MOMENT ON ENDLESS ELLIPTIC CYLINDER

[Width 8 inches, thickness 2 inches, air speed 40 miles per hour]

Angle of attack α , degrees	Lift	Drag	Moment about long axis pound foot per foot run	
	Pound per foot run		Experimental	Theoretical $N=1.3392 \sin 2\alpha$
-8	-2.30	0.160	-0.335	-0.3891
-6	-1.94	.139	-.254	-.2784
-4	-1.42	.122	-.170	-.1884
-3	-1.11	.116	-.127	-.1400
-2	-.76	.111	-.084	-.0934
-1	-.40	.108	-.042	-.0467
0	0	.106	0	0
+1	+.41	.108	+.044	+.0467
2	.80	.111	.085	.0934
3	1.12	.116	.129	.1400
4	1.44	.123	.171	.1884
5	1.90	.140	.249	.2784
+8	+2.16	.165	+.325	+.3891

*As the test angles α were in part fractional, all measurements in Table IX are faired from the original graphs of lift, drag, and moment versus α , in fig. 15.

TABLE X
LIFT, DRAG, AND MOMENT ON ENDLESS THIN FLAT PLATE

[Width 5 inches, air speed 40 miles per hour]

Angle of attack α , degrees	Lift	Drag	Moment about long axis pound foot per foot run	
	Pound per foot run		Experimental	Theoretical $N=0.5681 \sin 2\alpha$
-8	-1.345	0.190	-0.107	-0.1538
-6	-.980	.112	-.097	-.1160
-5	-.827	.0816	-.083	-.0984
-4	-.614	.0590	-.061	-.0777
-3	-.471	.0464	-.050	-.0583
-2	-.315	.0360	-.032	-.0389
-1	-.187	.0324	-.016	-.0195
0	0	.0312	0	0
+1	+.185	.0328	+.017	+.0195
2	.311	.0360	.033	.0389
3	.471	.0472	.050	.0583
4	.639	.0642	.066	.0777
5	.831	.0800	.085	.0984
6	1.018	.124	.098	.1160
8	1.345	.206	.107	.1538
10	1.538	.291	.084	+.1909
12	1.594	.360	.074	
14	1.532	.422	.050	
16	1.381	.480	.033	
+18	+1.530	.542	+.046	

TABLE XI
LIFT, DRAG, AND MOMENT ON THIN ELLIPTIC WING

[Length 30 inches, width 5 inches, air speed 40 miles per hour]

Angle of attack α degrees	Lift	Drag	Moment about long axis, pound foot	
	Pounds		Experimental	Theoretical $L=0.5963 \sin 2\alpha$
-8	-2.415	0.426	-0.173	-0.2471
-6	-1.835	.265	-.154	-.1863
-4	-1.186	.169	-.109	-.1247
-3	-.886	.138	-.082	-.0937
-2	-.587	.116	-.053	-.0625
-1	-.294	.105	-.031	-.0313
0	+.005	.108	0	0
+1	.306	.106	+.030	+.0313
2	.630	.118	.056	.0625
3	.890	.136	.084	.0937
4	1.195	.168	.111	.1247
6	1.861	.265	.156	.1863
8	2.474	.422	.185	.2471
10	2.865	.567	.134	+.3066
12	2.958	.696	.109	
14	2.892	.798	.094	
16	2.859	.897	.086	
18	2.789	.974	.097	
+20	+2.725	1.065	+.095	

TABLE XII
MOMENT ON PROLATE SPHEROID¹

[Length 24 inches, diameter 6 inches, through-air speed 40 feet per second]

Angle of attack α degrees	Moment about minor axis, pound foot			
	Measured on balance	Found by pressure integration		Theoretical $M=0.358 \sin 2\alpha$
		Rectilinear motion	Curvilinear motion	
-20	-0.179	-0.207	-0.157	-0.249
-10	-.108	-.122	-.078	-.133
-4	-.045	-.052	-.018	-.054
0	0	0	+.021	0
+10	+.108	+.122	+.127	+.133
+20	+.179	+.207	+.177	+.249

¹ Data taken from Reference 3.